AAPS PharmSciTech (2019) 20: 164
DOI: 10.1208/s12249-019-1362-7

Check for updates

Review Article

Theme: Advancements in Dissolution Testing of Oral and Non-Oral Formulations
Guest Editor: Sandra Klein

In Vitro Drug Dissolution/Permeation Testing of Nanocarriers for Skin Application: a Comprehensive Review

Ravi Sheshala,[1] Nor Khaizan Anuar,[1,2] Nor Hayati Abu Samah,[1] and Tin Wui Wong[2,3]

Received 5 December 2018; accepted 7 March 2019; published online 15 April 2019

Abstract. This review highlights *in vitro* drug dissolution/permeation methods available for topical and transdermal nanocarriers that have been designed to modulate the propensity of drug release, drug penetration into skin, and permeation into systemic circulation. Presently, a few of USFDA-approved *in vitro* dissolution/permeation methods are available for skin product testing with no specific application to nanocarriers. Researchers are largely utilizing the in-house dissolution/permeation testing methods of nanocarriers. These drug release and permeation methods are pending to be standardized. Their biorelevance with reference to *in vivo* plasma concentration–time profiles requires further exploration to enable translation of *in vitro* data for *in vivo* or clinical performance prediction.

KEY WORDS: *in vitro* dissolution; *in vitro* permeation; nanocarrier; skin; topical; transdermal.

SKIN

The skin is the largest human organ which accounts for 10 to 15% of body mass and covers nearly 2 m^2 of the body (1–3). The primary function of the skin is to act as a physical barrier that protects all other tissues from the external environment, infections, and excessive water loss. In addition, the skin helps to regulate body temperature and acts as the primary sensory organ. The full thickness of human skin consists of three principal layers: epidermis, dermis, and hypodermis. The epidermis is the outermost layer of skin constituting primarily of keratinocytes and is nourished by blood capillaries located in the dermis (1). The topmost epidermal layer is known as the stratum corneum (horny layer). The stratum corneum is a nonviable epidermis of 10 to 20 μm thick and composes of dead, flattened, keratin-rich cells, known as corneocytes (2,4). The corneocytes are surrounded by a cell envelope stabilized by cross-linked proteins and covalently bound lipids. These lipids are comprised of ceramides, free fatty acids, and cholesterol. The lipids and proteins located in this layer restrict the diffusion of most molecules due to the nature of their structural organization resembling a "brick and mortar," thus rendering the stratum corneum as the primary absorption barrier of the skin (2). The stratum corneum constitutes only 10% of the entire skin structure. Nonetheless, it represents a significant cutaneous barrier to exogenous compounds specifically those polar in nature.

DRUG DIFFUSION PATHWAYS

Generally, there are three potential routes of passive transport of drug molecules, from the surface of the skin to reach the subepidermal tissue region: (I) transappendageal, (II) transcellular route and (III) intercellular pathway (2).

The transappendageal or shunt route involves the diffusion of drugs into the skin through sweat gland pores (diameter 40–80 μm) (5) and hair follicle orifices (diameter 50–150 μm) (6). The drugs can directly reach the dermis without having to traverse through the stratum corneum. Hydrophilic and high molecular weight drug molecules, as well as particulate drug delivery systems such as liposomes, can adopt to the follicular penetration route (1,7–10). The follicular penetration is promoted by the movement of hair follicles which acts as a geared pump due to the zigzag structure of the cuticular layers along the hair shaft. The density of the skin appendages varies according to the body regions (10). The fractional area offered, however, is minimal and not more than 0.1% (1,2).

The intercellular pathway has the drugs diffused through the continuous lipid domains of the stratum corneum between the corneocytes and/or their surrounding aqueous pores into

Guest Editor: Sandra Klein

[1] Department of Pharmaceutics, Faculty of Pharmacy, Universiti Teknologi MARA Selangor, Puncak Alam Campus, 42300, Bandar Puncak Alam, Malaysia.
[2] Non-Destructive Biomedical and Pharmaceutical Research Centre, iPROMISE, Universiti Teknologi MARA Selangor, Puncak Alam Campus, 42300, Bandar Puncak Alam, Malaysia.
[3] To whom correspondence should be addressed. (e–mail: wongtinwui@salam.uitm.edu.my)

the viable epidermis and dermis. This route is considered to be the predominant pathway for the penetration of exogenous compounds through the skin (1,9). Most lipophilic drugs are absorbed *via* the intercellular pathway. This pathway is tortuous and indeed longer in distance than the thickness of the stratum corneum (4). The transcellular route is often regarded as a penetration pathway for small polar drugs (11). The drugs diffuse through the corneocytes passing through aqueous pores as well as partitioning into the lipid layers by interacting with their hydrophilic domains.

ANATOMICAL AND PHYSIOLOGICAL SKIN BARRIERS

The epidermal thickness and its hydration level as well as hair follicle density dictate the drug penetration capacity across the skin (12,13). Further, the pH, enzymatic activity, and microflora of the skin can negate the physicochemical stability of drugs, thereby reducing their therapeutic effectiveness. The pH of human skin typically ranges from 4.5 to 5.0 in the outer part of the stratum corneum and approaches neutrality in the lower part of the stratum corneum (14,15). The acidic characteristics of the stratum corneum may bring about drug degradation or unfavorable changes in its physicochemical properties which in turn reduces drug diffusion and absorption. The viable epidermis is composed of lytic enzymes (15,16). The spectrum and metabolic reactions of the enzymes are comparable to those found in other tissues such as the liver. However, the skin enzymatic activity is low, typically at 10% of the liver. A variety of endogenous enzymes such as proteases, lipases, and hyaluronidase are present in the extracellular compartment of the stratum corneum, sebaceous glands, and near hair follicles. The level of enzymatic activity varies with different anatomical sites of the skin (1). Healthy human skin is colonized by a range of microorganisms including *staphylococci*, *micrococci*, and *propionibacterium* (17). The skin flora possesses a wide range of enzymes capable of metabolizing topically applied molecules.

NANOCARRIERS FOR TOPICAL AND TRANSDERMAL DELIVERY

The United States Food and Drug Administration (USFDA) stated two "points to consider" in determining whether an FDA-regulated product involves the application of nanotechnology: (I) whether a material or end product is engineered to have at least one external dimension or an internal or surface structure, in the nanoscale range (approximately 1 to 100 nm); or (II) whether a material or end product is engineered to exhibit properties or phenomena, including physical or chemical properties or biological effects, that are attributable to its dimension(s), even if these dimensions fall outside the nanoscale range, up to 1 μm (1000 nm) (18). In this review, the terms nanomedicines, nanomaterials, nanoparticles, nanocarriers, and nanopharmaceuticals refer to entities that conform to the FDA's "points to consider."

Nanocarriers are defined as entities that are constructed using nanomaterials which add additional functionality to the active drug (19). They span a variety of structures including nanocrystals, nanosuspensions, nanoemulsions, liposomes, micelles, and polymer-based nanoformulations (19,20). With reference to skin drug delivery, the nanocarriers modulate the drug performance topically (on or into the skin strata) or transdermally (systemic exposure upon drug penetration through skin layers) over conventional dosage forms by offering features such as improved aqueous solubility and increased specific surface area as well as site-targeted delivery of drugs. Nanocarriers can be made of natural polysaccharides derived from various sources, such as algae (alginate), plants (pectin), microbes (dextran, xanthan gum), and animals (chitosan) (21). They can be made up of physiological lipids that are biodegradable and considered as well tolerated at the cellular level (22). Loading of drugs in nanocarriers protects them from premature chemical and enzymatic degradation (21).

The skin drug delivery by means of nanocarriers is mediated *via* several mechanisms, namely (I) the drug molecules are first released from the nanocarriers at the skin surfaces followed by drug diffusion into the skin, (II) the drug-loaded nanocarriers fuse with the stratum corneum at the skin–air interface and release the drug molecules into the skin thereafter, (III) the drug-loaded nanocarriers penetrate into the skin and release the drug at deeper skin layers, or (IV) a combination of any (1,23). The topical drug delivery involves the accumulation of the drug and/or nanocarriers at the epidermis and/or dermis layers, whereas transdermal drug delivery has the drug and/or nanocarriers permeated into the systemic circulation.

Size is regarded as one of the parameters influencing the penetration depth of nanocarriers through the skin (8,24,25). Being nano in size, the nanocarriers may traverse deeper into the skin and facilitate the transport of drug molecules through the skin tissue (1,26). It has been suggested that nanocarriers with dimensions < 20 nm may penetrate or permeate intact skin (2), nanocarriers < 45 nm may penetrate the damaged skin, and larger particles may be translocated or stored in the skin appendages (25). The nanocarriers possess a large surface area-to-volume ratio (21,27). They can transport a large amount of therapeutic cargo with a lesser volume (28). The drug loading and release profiles of nanocarriers can be easily tuned by altering their material composition and physical characteristics. The smart nanocarriers, comprising of stimulus-responsive building blocks as a part of the polymeric structure, can be designed to release drugs in response to skin microenvironmental stimuli such as temperature and pH as a function of skin diseases (1,29). Alternatively, the nanocarriers may serve as a skin depot releasing the encapsulated drug molecules over time (26). The nanocarriers can be decorated with targeting ligands for site-specific drug delivery (30). The pharmacokinetics and tissue biodistribution of drugs can be altered with the aim of maximizing the therapeutic effects and reducing the adverse effects of the drugs, specifically with reference to cancer treatments (1,3). Further, the nanocarriers can also be formulated to release drugs in a controlled manner by creating reservoirs in the skin to enhance localized therapeutic effects without developing systemic adverse effects (23,31).

IN VITRO DRUG DISSOLUTION TESTS OF NANOCARRIERS

The clinical bioavailability, efficacy, and safety of active molecules are associated with their *in vitro* performance with respect to drug dissolution and release (32–34). As stated in the USFDA guidance for industry 2017 (35), a fully validated *in vitro* drug dissolution/release testing serves as an essential tool to assess the quality of a drug product and to predict its *in vivo* performance (Fig. 1). *In vitro* dissolution test measures the drug release from nanocarriers as a function of time under a standardized setup (*e.g.*, type of membrane, temperature, pH and volume of dissolution media, agitation/rotation speed, and surfactant type and concentration) which simulates the body conditions (35). Depending on drug solubility, the dissolution medium may need to contain alcohol or surfactant. The dissolution test may be conducted without a synthetic membrane support as a function of drug product characteristics. In the case of topical and transdermal drug products, the dissolution test temperature and pH are typically set at 32 ± 1°C and 5.5, respectively, to reflect the normal skin surface temperature and pH (37–39). A temperature of 37°C, however, may be used in the case of vaginal products.

Between 1970 and 2015, a total of 359 applications for drug products containing nanomaterials were submitted to the Center for Drug Evaluation and Research within the FDA (30). Of these, approximately 4% of the submission is intended for topical application. However, only several submissions successfully gained regulatory approval (Table I). Pharmacopeial testing of pharmaceutical products is a fundamental requirement for most regulatory submissions around the world to ensure product quality, safety, and efficacy. Pharmacopeial monographs such as the US Pharmacopeia-National Formulary (USP/NF), the European Pharmacopoeia (EP), the Japanese Pharmacopoeia (JP), and the British Pharmacopoeia (BP) provide standardized drug dissolution methods and specifications for conventional dosage forms. The methods of drug dissolution differ from drug permeation measurement (45). The latter uses a biological tissue or a cell line instead of a synthetic membrane as the interface between the dosage form and the simulated systemic circulation. The standard tests are essential to provide regulatory authorities with the necessary data to allow a better correlation between *in vitro* and *in vivo* settings. To the best of our knowledge, compendial standards are available to assess the drug dissolution/permeation profiles of topical and transdermal dosage forms but with no specific applications to nanocarriers or nanomedicine.

DRUG DISSOLUTION METHODS FOR TOPICAL AND TRANSDERMAL NANOCARRIERS

The present compendial apparatus such as paddle over disk/disk assembly method (USP apparatus 5/EP 2.9.4.1), rotating cylinder (USP apparatus 6/EP 2.9.4.3), reciprocating disk (USP apparatus 7), and paddle over extraction cell method (EP 2.9.4.2) have been used for analyzing the drug dissolution profiles of transdermal products (38). In the case of semisolid topical dosage forms, the drug release rate profiles have been attained using the apparatus listed in USP Chapter <1724> namely vertical diffusion cell (Franz cell), immersion cell, and flow-through cell (USP apparatus 4) (46). With reference to topical and transdermal nanocarriers, there are no official compendial methods. The following sections highlight experimental approaches related to *in vitro* drug dissolution testings that have been adopted at the laboratory level for nanocarriers administered *via* the skin.

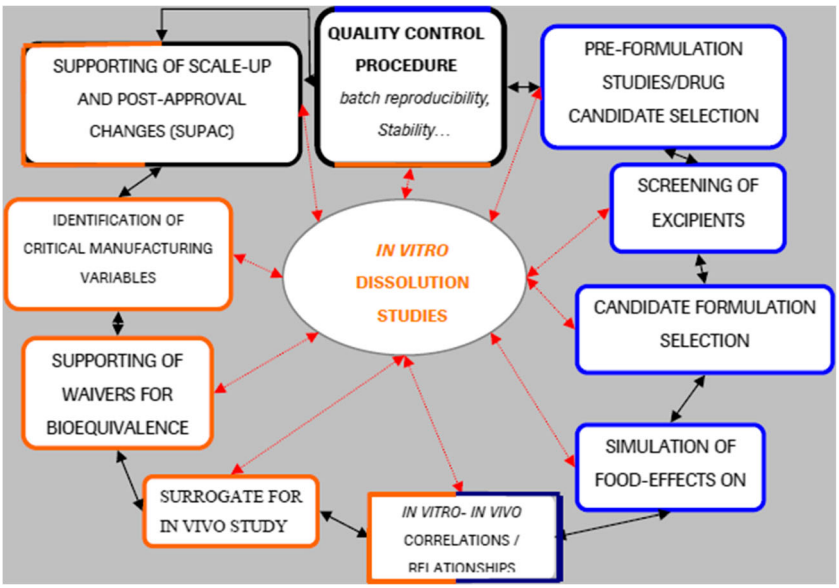

Fig. 1. The central roles of *in vitro* dissolution testing (early phases of product development shaped in blue, late phases in orange, market phase in black; dotted red arrows show the interplay of dissolution and black arrows show the interaction between the different development phases). Adopted from Scheubel (36) with reprint permission

Table I. Marketed Topical and Transdermal Nanomedicines

Product name	Drug	Dosage form/route	Therapeutic indication	Nanocarrier	Year of approval/ regulatory agency	Manufacturer (country)	Reference
Estrasorb™	Estradiol hemihydrate	Emulsion/transdermal	Moderate to severe vasomotor symptoms due to menopause	Micellar nanoparticles	2003/FDA	Novavax, Inc. (USA)	(30,40–42)
Elestrin™	Estradiol	Gel/transdermal	Moderate to severe vasomotor symptoms due to menopause	Calcium phosphate-based nanoparticles	2006/FDA	BioSanté Pharmaceuticals, Inc. (USA)	(30,40,41)
LMX®4 (previously known as ELA-Max)	Lidocaine	Cream/topical	Local anesthetic to provide skin surface anesthesia prior to venous cannulation or venipuncture	Liposome	2007/Medicines and Healthcare Products Regulatory Agency (MHRA)	Ferndale Pharmaceuticals Ltd. (USA)	(36,43)
Ameluz®	Aminolevulinic acid hydrochloride	Gel/topical	Treatment of actinic keratosis of mild to moderate intensity of the face and scalp	Nanoemulsion	2016/FDA	Biofrontera Bioscience GmbH (Germany)	(9,44)

Membrane-Free Dissolution Method

The membrane-free method is simple and a direct approach to determine the drug release from the nanoparticulate systems. In membrane-free methods, nanocarriers are directly introduced into the release medium maintained at a constant temperature. Drug release is assessed by physically separating the nanocarriers from the release media at predetermined time intervals *via* sample separation techniques (filtration/centrifugation/centrifugal ultrafiltration), and drug amount in the filtrate/supernatant is subsequently quantified using a suitable analytical technique (47,48).

Sabitha *et al.* (49) investigate *in vitro* drug dissolution profiles of 5-fluorouracil–loaded chitin nanogels at two different pH conditions, namely physiological (pH 7.4) and acidic (pH 4.5), with the latter simulating the skin or tumor site. The test proceeds by dispersing the pelleted samples freely in the dissolution medium at 37°C and subjecting to shaking at 50 rpm. Aliquots are withdrawn at specified time intervals and assayed for dissolved drug content. Fresh dissolution medium is replaced when applicable to maintain the sink test condition.

The USP paddle method type II dissolution apparatus has been employed to investigate the *in vitro* release rate of skin product in a membrane-free manner (50,51). Phosphate buffer pH 5.5 or 7.4 is used as the dissolution medium with its temperature being kept at 32 ± 0.5°C and stirring speed at 50 rpm.

Modified USP Dissolution Apparatus

Elmowafy *et al.* (52) analyze indomethacin release from nanocapsules and nanospheres using a modified USP dissolution apparatus (type I) which is also known as a glass basket dialysis method. The basket is replaced with a cylindrical glass tube (2.5 cm in diameter and 6 cm in length with a surface area of 4.9 cm^2) which is tightly covered with a cellulose acetate membrane (molecular weight cutoff diameter 12,000–14,000 Da) at the bottom and attached to a basket shaft (Fig. 2). About 2 mL of test formulations are placed in the cylindrical tube and dipped into 200 mL phosphate buffer saline pH 7.4. The apparatus temperature is maintained at 32 ± 0.5°C with a constant stirring speed of 100 rpm.

USP dissolution paddle method (type II) has been adopted by Kelidari *et al.* (54) and Moazeni *et al.* (55) to examine the drug dissolution behavior of spironolactone and fluconazole-loaded solid lipid nanoparticles, respectively (23,24) and Somagoni *et al.* (56) from the nanomiemgel containing aceclofenac and capsaicin (Fig. 2). Kelidari *et al.* (54) place the solid lipid nanoparticles directly into dissolution vessels containing the simulated intestinal fluid pH 6.8 (900 mL) of which it is maintained at 37°C with a paddle rotation speed of 60 rpm. The USP dissolution method resembles the membrane-free dissolution method. Moazeni *et al.* (55), on the other hand, introduce the solid lipid nanoparticulate dispersion into a dialysis bag (molecular weight cutoff diameter 12500 Da) and have it placed in 500 mL of simulated intestinal fluid pH 6.8. Prior to drug assay, the aliquots withdrawn are subjected to membrane

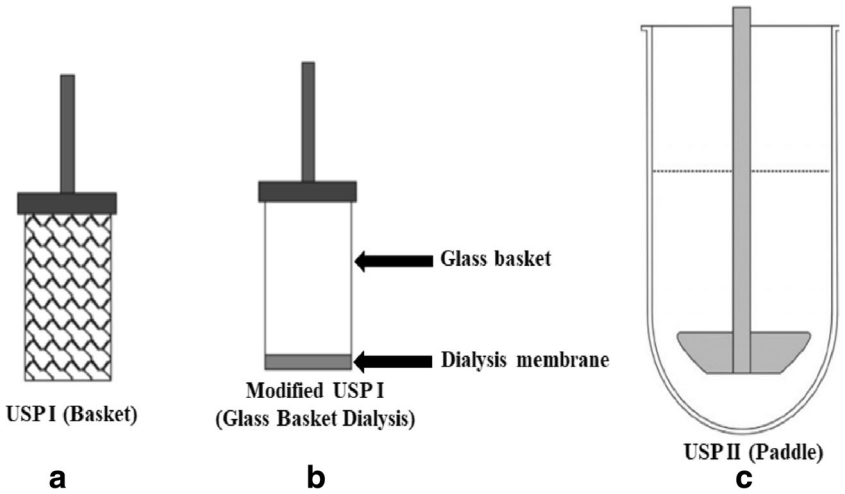

Fig. 2. Schematic representations of USP dissolution apparatus: **a** type I (basket) and **b** modified type I [adopted from D'Souza (47), copyright permitted for unrestricted use in any medium] and **c** type II (paddle) [adopted from Jug *et al.* (53) with reprint permission from Elsevier]

filtration (pore size 0.22 μm) and centrifugation (30 min at 25,000 rpm) to isolate fractions with dissolved drugs (23,24). Somagoni *et al.* (56) adopted a similar protocol as Moazeni *et al.* (55) where the nanoformulations are introduced in a cellulosic dialysis bag (molecular weight cutoff diameter 12,000 Da). With reference to the membrane-free method, the nanocarriers are present in the aliquots. Processing of aliquots by centrifugation or alternative separation techniques may lead to drug leaching from the nanocarriers. The extent and rate of drug release may be overestimated.

Membrane-Modeled Dissolution Method

In view of the complications of the membrane-free method, the membrane-modeled dissolution method is devised to reduce the probability of nanocarriers entering into the aliquots. Divya *et al.* (57) and Panonnummal *et al.* (58) contain the chitin-based nanogels in a cellophane membrane prior subjecting them to drug dissolution test as per the membrane-free method. Through the use of a membrane barrier, the donor (internal space of membrane tubing) and receptor (external space of membrane tubing) compartments are availed and the choice of the dissolution medium in the donor and receptor compartments may be varied. Divya *et al.* (57) disperse the nanogel pellets in donor fluid constituting pH 5.5 buffer and introduce it into a receptor fluid containing a mixture of pH 5.5 buffer and methanol (7:3) for acitretin and pH 5.5 buffer alone for aloe emodin. Panonnummal *et al.* (58), on the other hand, use phosphate buffer saline–ethanol mixture (7:3) as the receptor fluid. The organic solvent is introduced into the receptor fluids with the aim to promote drug solubilization and ease its chemical assay. Membranes such as cellophane (57–59) and cellulose (60,61) have been used with critical pore sizes not less than the molecular dimension of the dissolved drugs. Similar experimental approaches are also adopted by various researchers for investigating the dissolution characteristics of co-delivery of clobitasol propionate and calcipotriol (59), loperamide (60), benzocaine (61), amphotericin B (62), miconazole nitrate (63), and triptolide (64). A schematic representation of the membrane-modeled dissolution method is shown in Fig. 3.

The dialysis membrane has been used as the donor compartment with USP paddle method type II dissolution apparatus as the receptor compartment (66–72), apart from being left floating in a beaker or a stoppered glass vessel containing a receptor medium and stirred continuously at a specific temperature (73–75). Phosphate buffer pH 5.5 or 7.4 is used as the dissolution medium with its temperature typically being kept at 32 or 37°C and stirring speed at 50 to 500 rpm.

Diffusion Cell Method

Different types of diffusion cell apparatus, *i.e.*, horizontal, vertical, and flow-through diffusion cells have been used in assessing the drug dissolution profiles of nanocarriers (47). A typical apparatus is constituted of donor (top chamber) and receptor (bottom chamber) compartments which are partitioned by methylcellulose, nylon, cellophane, cellulose nitrate, or polysulfone membrane as the support of the skin products (76–79). The choice of membrane is governed by its pore size and composition to enable the released drug to diffuse into the receptor fluids (77). The membrane may be treated by soaking in isopropyl myristate to introduce the lipophilic property of the stratum corneum prior to mounting it onto the diffusion cell (78). Nonetheless, such treatment may complicate the drug dissolution with drug permeation due to the presence of a skin-like membrane. The sample (nanogels, solid lipid nanoparticles, nanoemulsion, nanostructured lipid carriers, and polymeric nanoparticles) is applied uniformly on the membrane surfaces facing the donor compartment (0.1–0.5 g). The dissolved drug passes through the membrane into the receptor compartment which is filled with a dissolution medium such as ethanol/water at 7:3 volume ratio, phosphate buffer pH 7.4, or a mixture of phosphate buffer saline pH 7.4 and Tween 80 or polysorbate 80 (76–78,80). The dissolution medium is introduced to the receptor compartment with care to avoid trapping the air

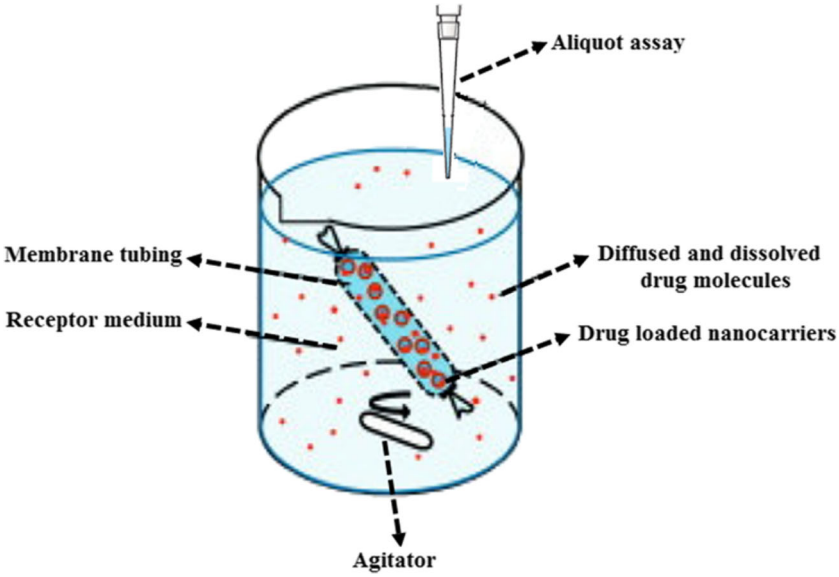

Fig. 3. Schematic representation of the membrane-modeled dissolution method. Adopted and modified from Deva Prasad (65) with reprint permission

pockets beneath the membrane which affect temperature distribution and drug diffusion from the top to the bottom chambers (8–10). The cell is maintained at a constant temperature of 32 to 37°C to simulate the temperature of human skin, and stirring speed is set at 600 to 800 rpm throughout the experiment. An aliquot of sample (200 to 400 μL) is collected from the receptor compartment *via* a sampling port at regular intervals for the quantification of drug release using suitable analytical techniques such as UV–visible spectrophotometry, high-performance liquid chromatography, and liquid chromatography–mass spectrometry.

Vertical diffusion cell is the most commonly used experimental apparatus to assess the drug release profiles of nanosized dosage forms (Fig. 4). It is available in different configurations such as the Franz diffusion cell, K–C cell (Keshary and Chien), and J–L cell (Jhawar and Lordi) (81,82). The vertical diffusion cell is constituted of amber or clear glass with the receptor compartment characterized by a

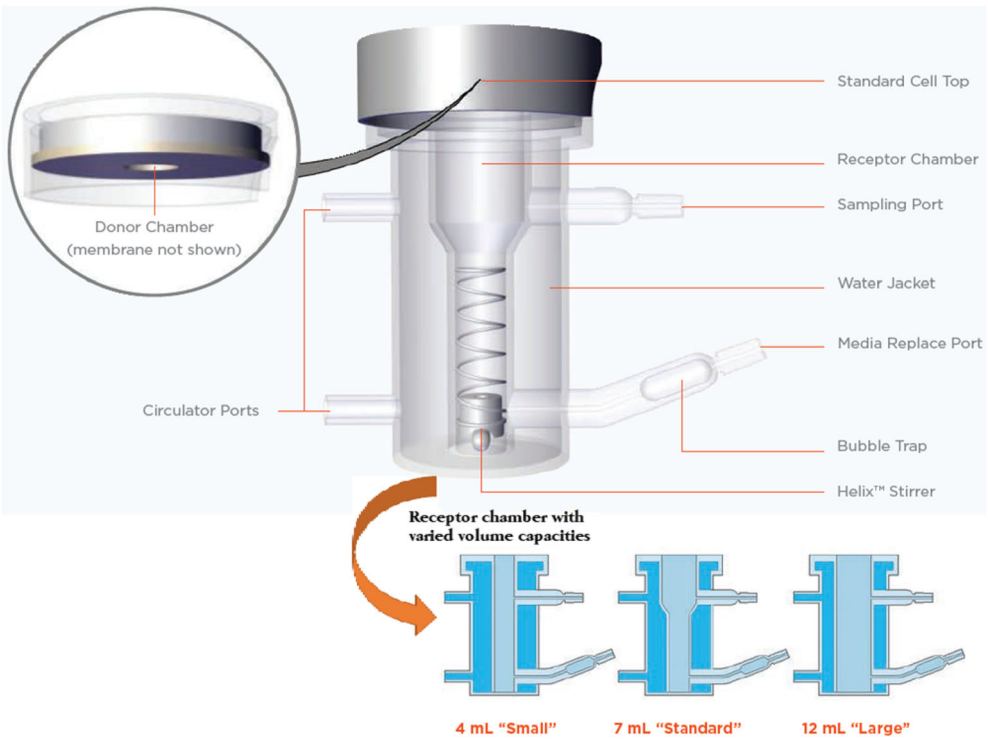

Fig. 4. Schematic representation of vertical diffusion cell with varied receptor chamber volume capacities (4, 7, and 12 mL). Hanson VDCs are compatible with synthetic, animal skin, cadaver skin, and Strat-M® membranes. Adopted from Teledyne Hanson Research (81) with reprint permission

customized volume capacity of 4, 7, or 12 mL. The Franz diffusion cell, with a receptor compartment volume of 10–12 mL, has an effective surface area of 1.5–5.0 cm^2. The receptor temperature is usually set to 32°C to reflect normal skin conditions. The J–L cell has 1 L USP dissolution vessel as a receptor compartment and an effective contact area of 12.6 cm^2. The J–L cell is developed to evaluate the drug dissolution profiles of suppositories. The K–C cell is developed with a receptor volume of 12 mL and a surface area of 3.14 cm^2. The K–C cell has the common apparatus configuration of vertical diffusion cell (Fig. 5) and is developed to overcome the limitation of Franz diffusion cells such as poor solution hydrodynamics, poor mixing, and temperature difference between donor and receptor compartments (83). The K–C cell is installed with a stirrer system within the receptor compartment to improve the efficiency of fluid mixing and increase the content homogeneity of the receptor compartment having larger volumes of dissolution medium (> 15 mL) (82). It assures sink condition and is critical in the evaluation of diffusion profiles of water-insoluble drugs.

Among all designs, the Franz diffusion cell is the most common apparatus used to examine the *in vitro* drug dissolution profiles of nanocarriers. Table II summarizes the types of drugs and nanocarriers and dissolution test parameters in association with skin dosage forms. With reference to Franz diffusion cell application, synthetic membranes such as polysulfone, cellulose, nylon, cellophane, cellulose nitrate impregnated with lauryl alcohol, dialysis membrane, or cellulose acetate in nature have been used as inert support of nanocarriers during the drug dissolution test. Phosphate buffer pH 5.5, 6.8, and 7.4, as well as HEPES buffer pH 7.4, had been used as the dissolution media. The dissolution medium is subjected to a wide range of stirring speed between 50 and 600 rpm. The alcohol and/or surfactant may be introduced in the receptor fluids to solubilize the released drugs for ease of drug assay, while a preservative may be added to retard the microbial growth in tests conducted over a prolonged duration. The nanocarriers may be applied directly or dispersed in a buffer solution prior to placing onto the membrane. The skin surface temperature and pH of human are 32°C and 5.5, respectively (106). The drug release is commonly referred to as fractional drug dissolved and deposited on the skin surfaces prior to its penetration into deep skin layers and permeation into the systemic blood circulation. With reference to the *in vitro* drug dissolution test of nanocarriers applied onto the skin, the dissolution tests nevertheless adopt human core body temperature and systemic circulation pH of 37°C and 7.4, respectively. These experimental conditions do not reflect the skin surface conditions. It brings about a misinterpretation about the dosage form performance specifically when pH-sensitive and/or temperature-dependent materials are used in the development of skin dosage forms.

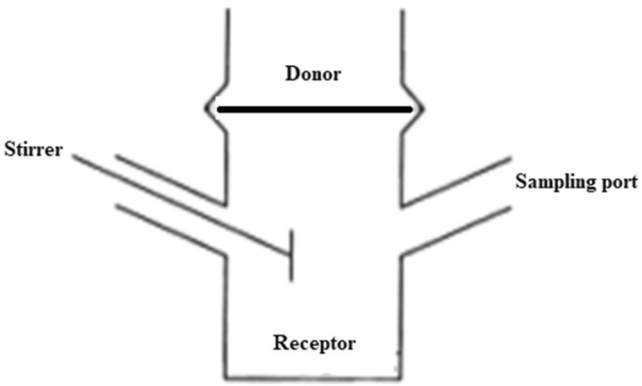

Fig. 5. Schematic diagram of the modified K–C diffusion apparatus. Adopted from Murthy and Hiremath (83) with reprint permission from Springer

Commercial Mini Dialysis Device

Inferring from diffusion cell and membrane-modeled dissolution methods, commercial mini dialysis devices are innovated with a unique polypropylene cup-like design at various volume capacities of 0.1, 0.5, and 2 mL (Fig. 6). The bottom of the cup is installed with a dialysis membrane with pore sizes corresponding to molecular weight cutoff diameters of 2000, 3500, 7000, 10,000, or 20,000 Da and low-binding regenerated cellulose membrane being used due to its good compatibility with common chemicals and buffer (107). Bose *et al.* (103) have performed the release study of quercetin formulated in the form of solid lipid nanoparticles using the commercial mini dialysis device. The sample is introduced into the cup which is denoted as the donor compartment. The mixture of distilled water and absolute alcohol at the volume ratio of 6.5:3.5 is used as the dissolution medium of the receptor compartment in the conical tube. The experiment is carried out at 37°C and a stirring speed of 100 rpm. The aliquot can be easily accessed from the receptor compartment, and replacement of fresh dissolution medium is possible. In comparison to the conventional membrane-modeled dissolution method, easy addition and removal of samples using standard laboratory pipettes and ease of testing multiple samples simultaneously with minimized amounts of dialysis buffer are the primary advantages of this innovation (107).

Drug-Selective Electrode Method

The drug-selective electrode method has been innovated to circumvent the major hurdles of membrane-modeled and membrane-free dissolution methods (108,109). The drug dissolution is conducted without the use of a dialysis membrane. It avoids drug–dialysis membrane interaction and adsorption which in turn prevents underestimation of the drug dissolution propensity and violation of the phenomenon of sink conditions due to the limitation imposed by the membrane. Using the drug-selective electrode method, the nanocarriers are freely available in a dissolution medium without any containment by a membrane, and the step of centrifugation can, however, be omitted as the drug assay is conducted *in situ* during the process of dissolution. The risks of overestimation of dissolved drug content can be reduced through reducing drug expulsion from delivery vesicles that are captured in the aliquot under the influence of centrifugal forces when the membrane-free method is concerned.

A schematic representation of the drug-selective electrode method is shown in Fig. 7. The test selectivity is brought about by drugs being electroactive. The method utilizes electrochemical analysis for measurement of drug release

Table II. *In Vitro* Drug Dissolution Studies of Skin Nanodosage Forms

Drug type	Carrier system	*In vitro* drug dissolution method					Reference
		Method	Membrane	Application mode of nanocarrier	Dissolution medium composition	Temperature/ agitation speed	
5-Fluorouracil	Nanogel	Membrane-free	No membrane	Nanogels are dispersed in phosphate buffer solution of pH 7.4 and 4.5	Phosphate buffer solution pH 7.4 and 4.5	37°C/50 rpm	(49)
Warfarin	Polymeric nanoparticles	Membrane-free	No membrane	Nanoparticles are placed directly in the dissolution medium	Phosphate buffer solution pH 5.5 or 7.4	32 ± 0.5°C/ 50 rpm	(50)
Ibuprofen	Micro-nanofiber matrices	Membrane-free	No membrane	Nanoparticles are placed directly in the dissolution medium	Acetate buffer solution pH 5.5	NI	(51)
Aceclofenac	Nanoparticles-in-gel	Membrane-modeled	Cellophane	Nanoparticles are suspended in phosphate buffer solution pH 7.4 and placed in the dialysis bag	Phosphate buffer solution pH 7.4	37 ± 1°C/ 100 rpm	(66)
Ropivacaine	Nanostructured lipid carrier	Membrane-modeled	Dialysis bag (molecular weight cutoff diameter 1000 Da)	Nanoparticles are placed in the dialysis bag	Phosphate buffer solution pH 7.4	32°C/ 100 rpm	(67)
Daidzein	Nanostructured lipid carrier	Membrane-modeled	Dialysis bag (molecular weight cutoff diameter 10,000 Da)	Nanoparticles are suspended in phosphate buffered saline pH 7.4 and placed in the dialysis bag	Phosphate buffered saline pH 7.4 containing 2% Tween	37 ± 0.5°C/ 100 rpm	(68)
Progesterone	Liquid crystalline nanoparticles	Membrane-modeled	Cellulosic dialysis membrane (molecular weight cutoff diameter 12,000–14,000 Da)	Nanoparticles are placed in the dialysis bag	Propylene glycol/ phosphate buffered saline pH 7.4 (2:3)	32 ± 0.5°C/ 100 rpm	(69)
Diclofenac diethyl amine	Polymeric nanoparticles	Membrane-modeled	Cellulose acetate (molecular weight cutoff diameter 12,000 Da)	Nanoparticles are placed in the dialysis bag	Phosphate buffer solution pH 7.4	37°C/NI	(70)
Ocimum sanctum L leaf extract	Nanostructured lipid carrier	Membrane-modeled	Dialysis bag	Nanoparticles are placed in the dialysis bag	Phosphate buffer solution pH 5.5	32 ± 0.5°C/ 50 rpm	(71)
Febuxostat	Niosomal gel	Membrane-modeled	Egg membrane	Nanoparticles are placed directly in the egg membrane	Phosphate buffer solution pH 7.4	37 ± 0.5°C/ 100 rpm	(72)
Pirfenidone	Polymeric nanoparticles	Membrane-modeled	Dialysis membrane (molecular weight cutoff diameter 12,000 Da)	Nanoparticles are dispersed in phosphate buffered saline and added into the dialysis membrane	Phosphate buffered saline pH 7.4	37 ± 0.5°C/ 100 rpm	(73)
Aceclofenac	Nanostructured lipid carrier	Membrane-modeled	Dialysis bag (molecular weight cutoff diameter 10,000–12,000 Da)	Nanoparticles are placed in the dialysis bag	Phosphate buffer solution pH 7.4:ethanol (70:30)	32 ± 0.5°C/ 500 rpm	(74)

Table II. (continued)

Drug type	Carrier system	*In vitro* drug dissolution method					Reference
		Method	Membrane	Application mode of nanocarrier	Dissolution medium composition	Temperature/ agitation speed	
Terbinafine	Nanoemulgel	Membrane-modeled	Dialysis bag (molecular weight cutoff diameter 12,000–14,000 Da)	Nanoparticles are placed in the dialysis bag	Mixture of methanol 10% and acetate buffer pH 5.5 (1:9)	37 ± 0.5°C/50 strokes per min	(75)
Acitretin and aloe emodin	Nanogel	Membrane-modeled	Cellophane membrane	Nanogel pellets are dispersed in pH 5.5 buffer prior to application onto the membrane	Acitretin:phosphate buffered saline pH 5.5 and methanol (7:3) Aloe emodin: phosphate buffered saline pH 5.5	37°C/50 rpm	(57)
Clobetasol	Nanogel	Membrane-modeled	Cellophane membrane	Nanogel suspension is added into one end of an open-end tube covered with dialysis membrane and the tube is introduced into the receptor compartment	Phosphate buffered saline–ethanol mixture (7:3) (pH 5.5 and 7.4)	37°C/50 rpm	(58)
Clobitasol propionate and calcipotriol	Nanoemulsion	Membrane-modeled	Cellophane membrane (molecular weight cutoff diameter 12,000 Da)	Dialysis bag is filled separately with clobitasol propionate and calcipotriol-loaded nanoemulsion and nanoemulsion gel, and then immersed individually in a glass vial containing 20 mL release medium	Phosphate buffered saline pH 5.8 and methanol (7:3)	37°C/50 rpm	(59)
Fluconazole	Solid lipid nanoparticles	USP dissolution apparatus II	Dialysis bag (molecular weight cutoff diameter 12,500 Da)	Drug-loaded solid lipid nanoparticulate dispersion is added into the dialysis bag and placed in 500 mL of dissolution medium	Simulated biological fluid pH 6.8	37 ± 0.1°C/ 60 rpm	(55)
Aceclofenac and capsaicin	Nanomiemgel (mixture of nanomicelle and nanoemulsion)	USP dissolution apparatus II	Cellulosic dialysis bag (molecular weight cutoff diameter 12,000 Da)	Formulation is placed in a dialysis bag and introduced into 500 mL of dissolution medium	Phosphate buffered saline pH 6.8	37 ± 0.5°C/ 100 rpm	(56)
Terbinafine hydrochloride	Solid lipid nanoparticles	Franz diffusion cell	Cellophane diffusion membrane (molecular weight cutoff diameter 12,000 Da)	The samples (plain drug solution, solid lipid nanoparticles, solid lipid nanoparticle-based gel, and commercial product) equivalent to 2 mg drug are	Phosphate buffer saline pH 7.4 containing 0.8% *v*/*v* of Tween 80	37.0 ± 0.5°C/NI	(76)

Table II. (continued)

Drug type	Carrier system	*In vitro* drug dissolution method					Reference
		Method	Membrane	Application mode of nanocarrier	Dissolution medium composition	Temperature/ agitation speed	
				kept onto the membrane in donor compartment			
8-Methoxypsoralen	Solid lipid nanoparticles and nanostructured lipid carriers	Franz diffusion cell	Cellulose membrane (Cellu-Sep® T2, molecular weight cutoff diameter 6000–8000 Da)	Nanoparticulate systems containing 8-methoxypsoralen are placed onto cellulose membrane in the donor compartment	Ethanol:pH 7.4 buffer (3:7)	37°C/600 rpm	(84)
Oleanolic and ursolic acids	Nanoemulsion	Franz diffusion cell	Dialysis membrane (molecular weight cutoff diameter 12,000–14,000 Da)	Oleanolic and ursolic acid nanoemulsions are placed onto the dialysis membrane in the donor compartment	Ethanol–water mixture (7:3)	32 ± 0.5°C/NI	(85)
Chitosan–carboxymethyl–5-fluorouracil–folate conjugate	Nanoparticles	Franz diffusion cell	Tuffryn membrane (pore size 0.45 μm)	The donor compartment was loaded with conjugated nanoparticles onto the membrane	Phosphate buffer pH 5.5	32 ± 2°C/ 400 rpm	(86)
5-Fluorouracil	Ethosomes	Franz diffusion cell	Tuffryn membrane (pore size 0.45 μm)	Ethosomes are loaded into the donor compartment	Phosphate buffer pH 5.5	32 ± 2°C/ 400 rpm	(87,88)
Miconazole nitrate	Ultra-small nanostructured lipid carrier	Modified Franz diffusion cell	Dialysis membrane (molecular weight cutoff diameter 12,000–14,000 Da)	Ultra-small nanostructured lipid carrier dispersion is placed onto the membrane	Phosphate buffer pH 7.4	32 ± 0.5°C/NI	(80)
Flavanones isolated from *Eysenhardtia platycarpa* leaves	Nanoemulsion and polymeric nanoparticles	Vertical Franz diffusion cell	Methylcellulose, nylon, and polysulfone membrane	Drug-loaded nanoemulsion is directly placed onto the membrane	Ethanol–water (7:3) mixture	32 ± 1°C/NI	(77)
Ibuprofen sodium and indomethacin	Nanostructured supramolecular hydrogel	Vertical Franz diffusion cell	Dialysis membrane (Cellu-Sep® T3, molecular weight cutoff diameter 12,000–14,000 Da)	Known weights of nanostructured supramolecular hydrogels are placed onto the dialysis membrane in the donor compartment and sealed with plastic paraffin film to prevent solvent evaporation	Ibuprofen:10 mM phosphate buffer saline pH 7.4 Indomethacin:ethanol	32°C/NI	(89)
Propranolol hydrochloride	Nanoparticles-in-mucoadhesive gel	Franz diffusion cell	Cellulose membrane	Nanoparticles are applied directly onto the membrane	Phosphate buffer solution pH 6.8	37 ± 1°C/NI	(90)
5-Fluorouracil	Polymeric nanoparticles	Franz diffusion cell	Polysulfone membrane	Nanoparticles are applied directly onto the membrane	Phosphate buffer solution pH 5.5	32 ± 2°C/ 400 rpm	(91)
Rabeprazole	Polymeric nanoparticles	Franz diffusion cell	Nylon membrane	Nanoparticles are suspended in phosphate buffer solution pH 7.4 prior to the application onto the membrane	Phosphate buffer solution pH 7.4	37°C/NI	(92)
Repaglinide		Franz diffusion cell	Cellophane membrane			37 ± 0.5°C/NI	(93)

Table II. (continued)

Drug type	Carrier system	*In vitro* drug dissolution method					Reference
		Method	Membrane	Application mode of nanocarrier	Dissolution medium composition	Temperature/ agitation speed	
	Polymeric nanoparticles			Nanoparticles are applied directly onto the membrane	Phosphate buffer solution pH 7.4		
Glibenclamide	Nanostructured lipid carrier	Franz diffusion cell	Cellophane membrane (molecular weight cutoff diameter 12,000 Da)	Nanoparticles are suspended in dissolution medium prior to application onto the membrane	Mixture of ethanol and phosphate buffer solution pH 7.4 (30:70)	37 ± 0.5°C/ 600 rpm	(94)
Flufenamic acid	Polymeric nanoparticles + iontophoresis	Franz diffusion cell	Regenerated cellulose membrane (molecular weight cutoff diameter 3500 Da)	Nanoparticles are suspended in dissolution medium prior to application onto the membrane	25 mM HEPES buffer pH 7.4 containing 154 mM sodium chloride	32°C/NI	(95)
Oxaprozin	Nanostructured lipid carrier	Franz diffusion cell	Cellulose nitrate impregnated with lauryl alcohol	Nanoparticles are applied directly onto the membrane	Phosphate buffer solution pH 7.4	32°C/50 rpm	(96)
Flufenamic acid and caffeine	Polymeric nanoparticles	Franz diffusion cell	Cellulose membrane (molecular weight cutoff diameter 12,000–14,000 Da)	Nanoparticles are suspended in phosphate buffer solution pH 7 prior to the application onto the membrane	Phosphate buffer solution pH 7	32°C/NI	(97)
Testosterone	Polymeric nanoparticles	Franz diffusion cell	Cellulose membrane (molecular weight cutoff diameter 12,000–14,000 Da)	Nanoparticles are suspended in phosphate buffer solution pH 7 containing 2% (*v*/*v*) Igepal® CA-630 (a nonionic polyethylene glycol derivative) and 0.4% (*v*/*v*) ethanol prior to application onto the membrane	Phosphate buffer solution pH 7 containing 2% (*v*/*v*) Igepal® CA-630 (a nonionic polyethylene glycol derivative) and 0.4% (*v*/*v*) ethanol	32°C/NI	(97)
Raloxifene hydrochloride	Nanotransfersome	Franz diffusion cell	Dialysis membrane (molecular weight cutoff diameter 10,000–14,000 Da)	Nanoparticles are applied directly onto the membrane	Phosphate buffer solution pH 7.4	32 ± 0.5°C/ 400 rpm	(98)
Diltiazem hydrochloride	Nanocomposite	Franz diffusion cell	Cellulose acetate	Nanoparticles are applied directly onto the membrane	Phosphate buffered saline (pH not indicated)	NI/50 rpm	(99)
Tadalafil	Nanoemulsion	Franz diffusion cell	NI	Nanoparticles are applied directly onto the membrane	Phosphate buffered saline pH 7.2	32 ± 0.5°C/ 400 rpm	(100)
Diclofenac	Polymeric nanoparticles	Modified Transwell insert	Strat-M membrane	Nanoparticles are applied directly onto the membrane	Phosphate buffer solution pH 7.4	32 ± 0.5°C/NI	(101)
Clonidine	Polymeric nanoparticles	Microcentrifuge tube	NI	Nanoparticles are placed directly in the microcentrifuge tube	Phosphate buffered saline pH 7.4 with	37°C/NI	(102)

Table II. (continued)

Drug type	Carrier system	*In vitro* drug dissolution method					Reference
		Method	Membrane	Application mode of nanocarrier	Dissolution medium composition	Temperature/ agitation speed	
				containing the dissolution medium	0.1% sodium azide and 0.1% Tween 80		
Vitamin A	Solid lipid nanoparticles	K–C diffusion cell	Cellulose nitrate membrane	Liquid nanoparticulate dispersion is applied onto the membrane	Phosphate buffered saline containing 3% polysorbate 80	NI	(78)
Quercetin	Solid lipid nanoparticles	Commercial mini dialysis devices	Cellulose membrane (molecular weight cutoff diameter 10,000 Da)	Quercetin-loaded solid lipid nanoparticle dispersion is added to the donor compartment	Mixture of distilled water and absolute alcohol (6.5:3.5)	37°C/100 rpm	(103)
Procaine hydrochloride and imipramine hydrochloride	Nanogel	Drug-selective electrode (potentiometric)	No membrane	Procaine hydrochloride and imipramine hydrochloride-loaded nanogel particles are added into a double-walled jacketed vessel containing 10 mM sodium chloride solution and 10 mM phosphate buffer solution, respectively	Procaine hydrochloride: 10 mM sodium chloride solution Imipramine hydrochloride:10 mM phosphate buffer solution	37°C/NI	(104)
Doxorubicin	Nanoparticles (liposomes)	Drug-selective electrode (repetitive square-wave voltammetric)	No membrane	Doxorubicin-loaded liposomes are added to a phosphate buffer at either pH 7.4 or 5.2	Phosphate buffer at either pH 7.4 or 5.2	NI	(105)

NI = not indicated

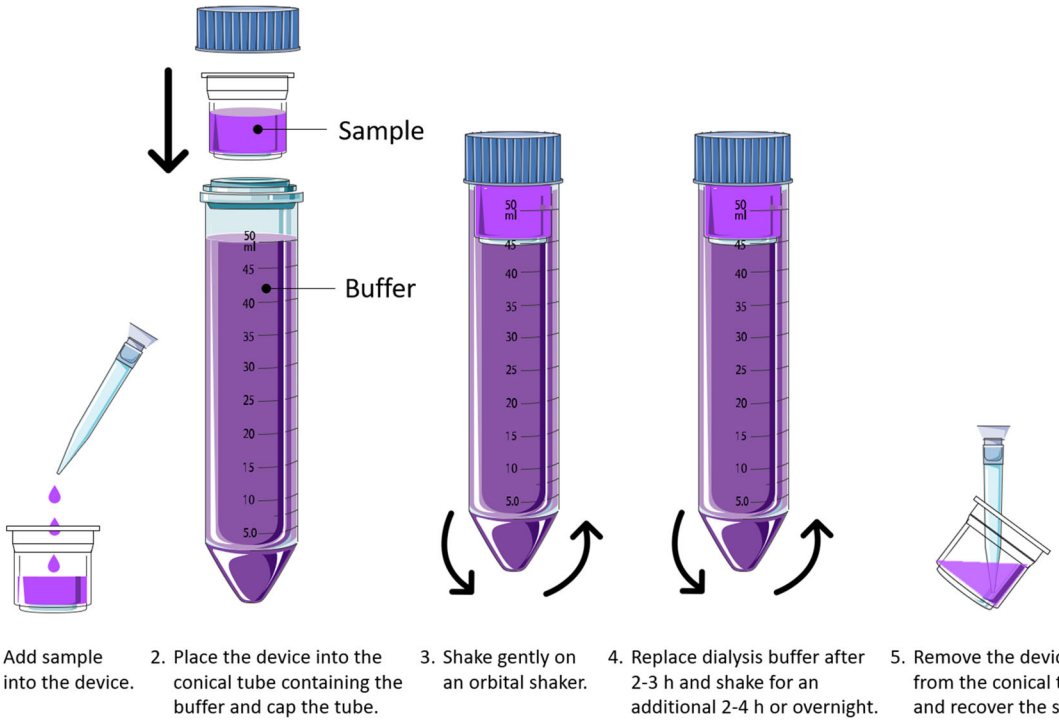

Fig. 6. Schematic representation of commercial mini dialysis device. Adopted and redrawn from Thermo Fischer Scientific (107)

under real-time conditions. A few approaches such as potentiometric (104), repetitive square-wave voltammetric (105), and differential pulse polarography (110,111) systems are used to assess real-time drug release directly and continuously from a dosage form. The drug-selective electrode method is limited to electroactive drugs, requires sensors specific to a particular drug, and is characterized by varying sensitivities and responses with each technique or in response to changes in pH or ionic strength of the dissolution medium (47,108). In general, the drug-selective electrode method is constituted of a double-walled jacketed vessel containing a dissolution medium where the drug-loaded nanocarriers are introduced for real-time measurement of drug release, working electrode, reference electrode, and counter electrode. The whole setup is kept constant at 37°C, and the dissolution medium is stirred continuously during the measurements. The drug selectivity is mediated *via* a voltameter, and electromotive force measurements are recorded.

Tan *et al.* (104) analyze procaine hydrochloride and imipramine hydrochloride release from methacrylic acid–ethyl acrylate nanogels using drug-selective electrode. The electrochemical system arrangement is Ag/AgBr/internal solution/membrane/test solution/Ag/AgCl reference electrode. The internal solution in a Teflon tubing contains 1 mM procaine hydrochloride or 1 mM imipramine hydrochloride and 10 mM sodium bromide. Procaine hydrochloride–loaded nanogel particles are added into a double-walled jacketed vessel containing 100 cm^3 10 mM

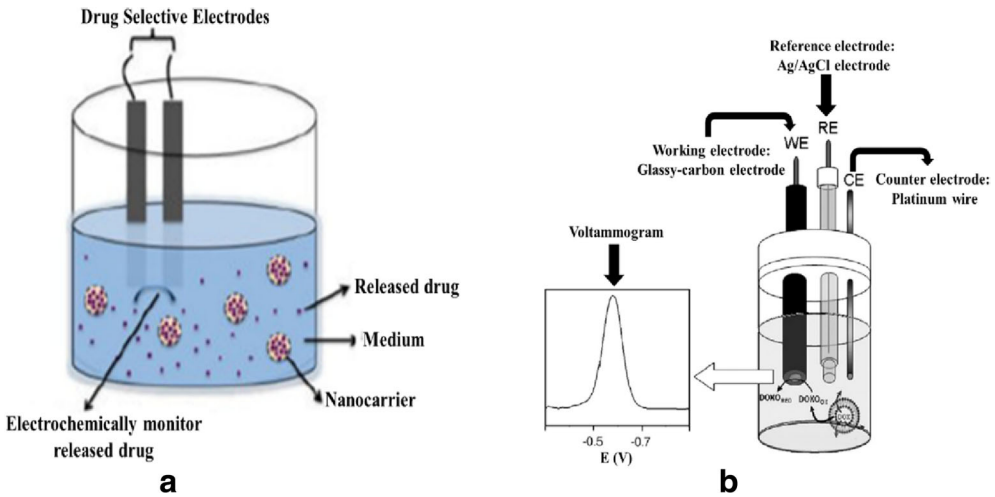

Fig. 7. Schematic representation of drug-selective electrode method where the drug release is monitored electrochemically. **a** Potentiometric [adopted from Shen and Burgess (48) with reprint permission] and **b** repetitive square-wave voltammetric [adopted from Mora *et al.* (105) with reprint permission]

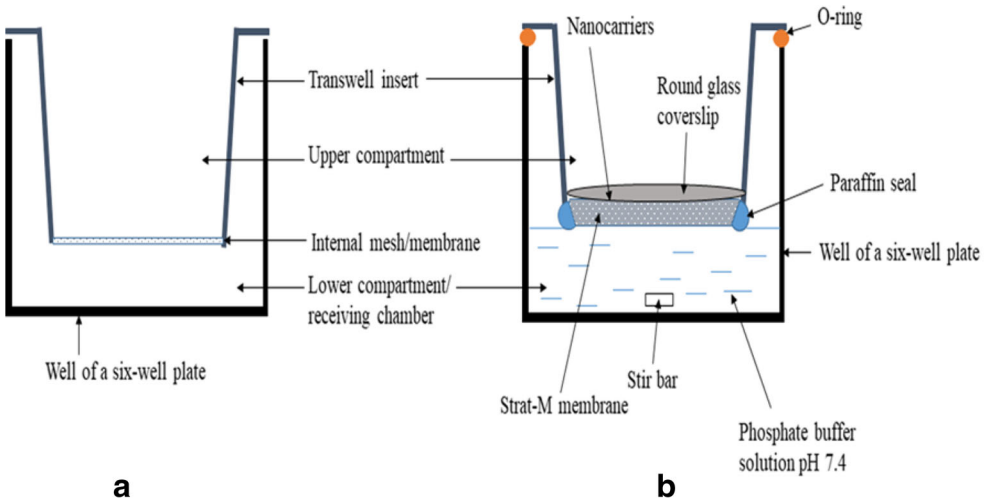

Fig. 8. Schematic representation of Transwell insert: **a** unmodified and **b** modified Transwell insert. Adopted and modified from Carmona-Moran *et al.* (101) with reprint permission

sodium chloride solution (test solution) and imipramine hydrochloride–loaded nanogel particles are added into 20 cm^3 10 mM phosphate buffer solution (test solution) at 37°C. A membrane disk of 12 mm in diameter is fixed onto the Teflon tubing of the electrode. Electromotive force measurements are recorded by the Radiometer ABU93 Triburette titration system with a built-in micro-voltameter at a regular interval of 5 min. According to Mora *et al.* (105), a repetitive square-wave voltammetric system comprises of a 5-mL electrochemical cell of which is constituted of a 2-mm diameter glassy-carbon working electrode, a 1-mm diameter platinum wire counter electrode, and an Ag/AgCl reference electrode. The cell is closed with a Teflon cover, and the test solution is bubbled with nitrogen. A square-wave voltammetry has been used to record the voltammograms of doxorubicin released from the liposomes at pH 7.4 over − 0.3 to − 0.9 V range. The differential pulse polarography system consists of an EG & G 303A static electrode mercury with an Ag/AgCl reference electrode, a platinum counter electrode, and an EG & G 264A polarographic analyzer (111). Polarograms of pyroxicam have been obtained over − 0.8 to − 1.8 V range.

Modified Transwell Insert

A modified Transwell diffusion system has been used to investigate the diclofenac transport from temperature-responsive nanogels (101). The Transwell diffusion system is constituted of an upper compartment and a lower compartment, separated by an internal mesh (Fig. 8). The internal mesh at the bottom of the Transwell insert is removed and replaced with a membrane such as Strat-M membrane. The small gap between the Transwell insert and the membrane is sealed using molten paraffin. The insert is placed in the well of a six-well plate. An O-ring is added between the Transwell insert and the well to raise the Transwell insert in the receiving chamber, enabling the receptor compartment to accommodate an increased volume of dissolution medium. Phosphate buffer solution pH 7.4 is used as the dissolution medium with its temperature and agitation speed kept at 32 ± 0.5°C and 100 rpm, respectively. The upper level of the buffer is constantly in contact with the bottom surfaces of the membrane. The nanocarriers are applied onto the top surfaces of the membrane within an insert. They are spread uniformly and covered with a glass coverslip to prevent

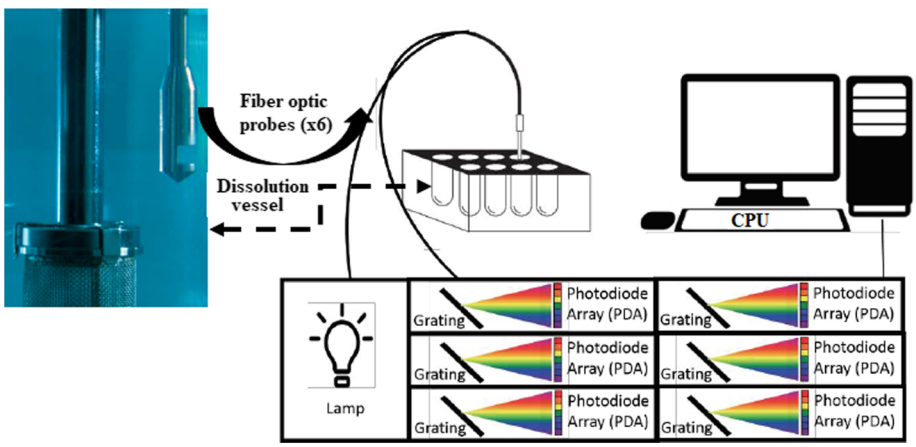

Fig. 9. Schematic diagram of *in situ* fiber optic probe dissolution system with photodiode array detector. Adopted and amended from Martin (112) and Nir and Lu (114) with reprint permission

Table III. *In Vitro* Drug Permeation Studies of Skin Nanodosage Forms

Drug type	Carrier system	Route	*In vitro* drug permeation method					Reference
			Method	Skin type	Application mode of nanocarrier	Permeation medium composition	Temperature/ agitation speed	
Spironolactone	Solid lipid nanoparticle	Topical	Franz diffusion cell	Abdominal rat skin	Lyophilized spironolactone solid lipid nanoparticles are dispersed in 5 mL distilled water and applied on the skin surface	Phosphate buffer saline pH 7.4	37 °C / 300 rpm	(54)
Clobetasol	Nanogel	Topical	Franz diffusion cell	Full-thickness porcine ear skin	An aliquot of nanogel suspension is added to the stratum corneum of the skin in the donor compartment	Mixture of ethanol and phosphate buffered saline pH 5.5 (3:7)	32 °C / 400 rpm	(58)
Clobitasol propionate and calcipotriol	Nanoemulsion	Topical	Franz diffusion cell	Pig ear skin	Clobitasol propionate–calcipotriol-loaded nanoemulsion and nanoemulsion gel are applied onto the skin surface in the donor compartment	Mixture of phosphate buffer saline pH 5.8 and methanol (7:3)	37°C/75 rpm	(59)
Terbinafine hydrochloride	Solid lipid nanoparticles	Topical	Franz diffusion cell	Full-thickness rat abdominal skin	The test formulations (solid lipid nanoparticle-based gel and commercial product) equivalent to 2 mg drug are applied onto the skin	Phosphate buffer saline pH 7.4 with 0.8% *v/v* Tween 80	37.0 ± 0.5°C/ NI	(76)
Flavanones isolated from *Eysenhardtia platycarpa* leaves	Nanoemulsion and polymeric nanoparticles	Topical	Franz diffusion cell	Abdominal human skin	The test formulation is applied directly onto the skin surface	Mixture of ethanol and water (7:3)	32 ± 1°C/NI	(77)
Miconazole nitrate	Ultra-small nanostructured lipid carrier	Topical	Franz diffusion cell	Goat cadaver skin	Ultra-small nanostructured lipid carrier gel formulation is directly applied onto the skin	Physiological saline pH 7.4	32 ± 0.5 °C/ 300 rpm	(80)
Psoralen	Solid lipid nanoparticle and nanostructured lipid carrier	Topical	Franz diffusion cell	Full-thickness mice skin	Nanoparticulate systems containing 8-methoxypsoralen are applied directly on the skin surface	Mixture of ethanol and buffer pH 7.4 (3:7)	37 °C / 600 rpm	(84)
Oleanolic and ursolic acids	Nanoemulsion	Topical	Franz diffusion cell	Abdominal human skin	Nanoemulsion is placed onto the donor compartment in contact with the outer surface of the skin	Mixture of ethanol and water (7:3)	32 ± 0.5°C/NI	(85)
5-Fluorouracil	Ethosomes	Topical		Abdominal rat skin				(87,88)

Table III. (continued)

Drug type	Carrier system	Route	*In vitro* drug permeation method					Reference
			Method	Skin type	Application mode of nanocarrier	Permeation medium composition	Temperature/ agitation speed	
			Franz diffusion cell		Ethosomal dispersion is applied onto the skin at the donor compartment	phosphate buffer saline pH 7.4 containing 0.01% *w/v* sodium azide	37 ± 2 °C / 400 rpm	
Fludrocortisone acetate and flumethasone pivalate	Nanoemulsion	Topical	Franz diffusion cell	Porcine abdominal skin	Nanoemulsion is gently placed on the skin membrane in the donor chamber	Phosphate buffer solution (pH 7.4, 0.012 M)	32°C/NI	(123)
Fludrocortisone acetate	Nanoemulsion	Topical	Franz diffusion cell	Porcine abdominal skin	The accurately weighted formulation is placed on the excised skin in the donor chamber	Phosphate buffer (pH 7.4, 0.012 M) and additives with buffer media containing 1.4% *w/v* of bovine serum albumin or 20% *v/v* of either propylene glycol, polyethylene glycol 400, or ethanol	32 ± 0.5°C/NI	(124)
Fludrocortisone acetate, flufenamic acid, fluconazole, and minoxidil	Nanoemulsion	Topical	Franz diffusion cell	Porcine abdominal skin	Nanoemulsion is placed on the excised skin in the donor chamber	Phosphate buffer pH 7.4	32°C/NI	(125)
Vitamin K1	Nanoemulsion	Topical	Franz diffusion cell	Porcine ear skin	A measured amount of nanoemulsion is poured or nebulized by nebulizer loaded with 1 mL of formulation onto skin membrane	Mixture of phosphate buffer solution and ethanol (7:3)	37 °C / 600 rpm	(126)
Quercetin	Nanostructured lipid carrier	Topical	Franz diffusion cell	Male Kunming mice	Quercetin loaded nanostructured lipid carrier suspension (1.0 mg/mL) is applied on the skin surface	Physiological saline with 1% Tween 80	32 ± 0.5 °C/ 600 rpm	(127)
Terbinafine and citral	Nanoemulsion	Topical and transdermal	Franz diffusion cell	Guinea pig abdominal skin	The donor chamber consisting of a skin membrane is filled with nanoemulsion and nanoemulsion gels	Phosphate buffer saline	37 ± 1 °C / 300 rpm	(128)
Lornoxicam	Nanoemulsion	Topical	Franz diffusion cell	Pig abdominal skin	Nanoemulsion, nanoemulsion gel, and conventional gel loaded with lornoxicam are placed on the skin membrane in the donor compartment	Phosphate buffer saline pH 7.4	37 ± 0.5 °C/ 800 rpm	(129)
Ketoprofen	Nanoemulsion	Topical	Franz glass diffusion cell	Mouse skin	Nanoemulsion is applied to the epidermal skin surface	Phosphate buffer solution pH 7.4 (0.01 M)	37 ± 0.5 °C/ 600 rpm	(130)

Table III. (continued)

Drug type	Carrier system	Route	*In vitro* drug permeation method					Reference
			Method	Skin type	Application mode of nanocarrier	Permeation medium composition	Temperature/ agitation speed	
Hydrocortisone and hydroxytyrosol	Polymeric nanoparticles	Topical	Franz diffusion cell	Full-thickness mouse skin	Drug-loaded nanoparticles are directly applied onto the surface of the skin	Mixture of phosphate buffered saline pH 7.4 and acetonitrile (7:3)	37 °C / 600 rpm	(131)
Naproxen	Solid lipid nanoparticles	Topical	Franz diffusion cell	Abdominal rat skin	Naproxen loaded solid lipid nanoparticles are applied onto the skin surface in donor chamber	50:50 ethanol/water mixture	37 ± 0.5 °C/ 300 rpm	(132)
Warfarin	Polymeric nanoparticles	Transdermal	Franz diffusion cell	Full-thickness rat skin	Nanoparticles are applied directly onto the skin	Phosphate buffer solution pH 7.4	37°C/NI	(50)
Aceclofenac	Nanoparticles-in-gel	Transdermal	Franz diffusion cell	Full-thickness mouse skin	Nanoparticles are applied directly onto the skin	Phosphate buffer solution pH 7.4 with 0.0025% *w/v* sodium azide	37 ± 0.5°C/NI	(66)
Ropivacaine	Nanostructured lipid carrier	Transdermal	Franz diffusion cell	Full-thickness mice skin	Nanoparticles are applied directly onto the skin	Phosphate buffer solution pH 7.4	32 ± 0.5°C/NI	(67)
Progesterone	Liquid crystalline nanoparticles	Transdermal	Franz diffusion cell	Rabbit ear skin	Nanoparticles are applied directly onto the skin	Propylene glycol/phosphate buffered saline pH 7.4 (2:3)	32 ± 0.5 °C/ 100 rpm	(69)
Ocimum sanctum L leaf extract	Nanostructured lipid carrier	Transdermal	Franz diffusion cell	Full-thickness rat skin	Nanoparticles are applied directly onto the skin	Permeation media	37 °C / 600 rpm	(71)
Febuxostat	Niosomal gel	Transdermal	Franz diffusion cell	Full-thickness rat skin	Nanoparticles are applied directly onto the skin	Phosphate buffer solution pH 7.4	NI/400 rpm	(72)
Pirfenidone	Polymeric nanoparticles	Transdermal	Franz diffusion cell	Full-thickness rat skin	Nanoparticles are applied directly onto the skin	Phosphate buffered saline pH 7.4	37 ± 0.5 °C/ 200 rpm	(73)
Aceclofenac	Nanostructured lipid carrier	Transdermal	Franz diffusion cell	Full-thickness porcine skin	Nanoparticles are applied directly onto the skin	Mixture of phosphate buffer solution pH 7.4 and ethanol (7:3)	32 ± 0.5 °C/ 500 rpm	(74)
Terbinafine	Nanoemulgel	Transdermal	Franz diffusion cell	Full-thickness rat skin	Nanoparticles are applied directly onto the skin	Mixture of 10% methanol and acetate buffer pH 5.5 (1:9)	37 ± 0.5°C/25 strokes per min	(75)
Propranolol hydrochloride	Nanoparticles dispersed in gel	Transdermal	Franz diffusion cell	Full-thickness porcine skin	Nanoparticles are applied directly onto the skin	Phosphate buffer solution pH 6.8	37 ± 1°C/NI	(90)
5-Fluorouracil	Polymeric nanoparticles	Transdermal	Franz diffusion cell	Full-thickness rat skin	Nanoparticles are suspended in acetate buffer pH 5 prior to the application onto the skin	Phosphate buffer solution pH 7.4 with 0.01% *w/v* sodium azide	37 ± 2 °C / 400 rpm	(91)
Rabeprazole	Polymeric nanoparticles	Transdermal	Franz diffusion cell	Full-thickness rat skin	Nanoparticles are applied directly onto the skin	Phosphate buffer solution pH 7.4	37°C/NI	(92)
Repaglinide	Polymeric nanoparticles	Transdermal	Franz diffusion cell	Full-thickness rat skin	Nanoparticles are applied onto the skin	Phosphate buffer solution pH 7.4	37 ± 0.2 °C/ 100 rpm	(93)
Glibenclamide	Nanostructured lipid carrier	Transdermal	Franz diffusion cell	Full-thickness rat skin	Nanoparticles are applied directly onto the skin	Mixture of ethanol and phosphate buffer solution pH 7.4 (30:70)	37 ± 0.5 °C/ 600 rpm	(94)
Flufenamic acid	Polymeric nanoparticles	Transdermal	Franz diffusion cell	Human epidermis and full-thickness porcine skin.	Nanoparticles are suspended in 25 mM	HEPES buffer (pH 7.4, 25 nM) containing 154 mM sodium chloride	32°C/NI	(95)

Table III. (continued)

Drug type	Carrier system	Route	*In vitro* drug permeation method					Reference
			Method	Skin type	Application mode of nanocarrier	Permeation medium composition	Temperature/ agitation speed	
				Regenerated cellulose dialysis membrane is used as a supportive membrane of human epidermis	HEPES buffer pH 7.4 containing 154 mM sodium chloride prior to the application onto the skin			
Oxaprozin	Nanostructured lipid carrier	Transdermal	Franz diffusion cell	Human epidermis	Nanoparticles are applied directly onto the skin	Phosphate buffer solution pH 7.4	32°C/50 rpm	(96)
Flufenamic acid, caffeine, and testosterone	Polymeric nanoparticles	Transdermal	Franz diffusion cell	Human epidermis	Nanoparticles suspended in phosphate buffer solution pH 7 prior to application onto skin	Phosphate buffer solution pH 7	32°C/NI	(97)
Raloxifene hydrochloride	Nanotransfersome	Transdermal	Franz diffusion cell	Full-thickness rat and rabbit skin	Nanoparticles are applied directly onto the skin	Phosphate buffer solution pH 7.4	32 ± 0.5°C/ 400 rpm	(98)
Curcumin	Polymeric nanoparticles	Transdermal	Franz diffusion cell	Full-thickness mice skin	Nanoparticles are applied directly onto the skin	Mixture of phosphate buffer solution pH 7.4 and absolute ethanol (1:1)	37 ± 0.5°C/ 400 rpm	(133)
Colchicine	Solid lipid nanoparticles	Transdermal	Franz diffusion cell	Full-thickness rat skin	Nanoparticles are applied directly onto the skin	Phosphate buffer solution pH 6.4	37 ± 0.5°C/NI	(134)
Curcumin and 5-fluorouracil	Polymeric nanoparticles	Transdermal	Franz diffusion cell	Rat epidermis	Nanoparticles are applied directly onto the skin	Phosphate buffered saline pH 7.4	37°C/ 750 rpm	(135)
Tetrahydrocurcumin	Nanofiber patch	Transdermal	Franz diffusion cell	Full-thickness porcine skin	Nanoparticles are applied directly onto the skin	Phosphate buffer solution pH 6.8 with 20% *v/v* ethanol	37 ± 0.5°C/ 300 rpm	(136)
Glimepiride	Ethosomal nanovesicles	Transdermal	Franz diffusion cell	Full-thickness rat skin	Nanoparticles are applied directly onto the skin	Phosphate buffer saline pH 7.4	32 ± 0.5°C/ 400 rpm	(137)
Lansoprazole	Nanostructured lipid carrier	Transdermal	Franz diffusion cell	Full-thickness rat skin	Nanoparticles are applied directly onto the skin	Carbonate buffer solution	37°C/ 700 rpm	(138)
Resveratrol	Nanostructured emulsion	Transdermal	Franz diffusion cell	Full-thickness rat skin	Nanoparticles are applied directly onto the skin	Phosphate buffered saline pH 7.4 containing 20% propylene glycol and 20% ethanol	37 ± 0.5°C/ 600 rpm	(139)
Ibuprofen	Nano-ethanolic liposome	Transdermal	Franz diffusion cell	Full-thickness rat skin	Nanoparticles are applied directly onto the skin	Mixture of ethanol and phosphate buffer solution pH 7.4	32 ± 0.2°C/ 600 rpm	(140)
Selegiline hydrochloride	Nanoemulgel	Transdermal	Franz diffusion cell	Full-thickness rat skin	Nanoparticles are applied directly onto the skin	Phosphate buffer solution pH 7.4	37 ± 1°C/ 100 rpm	(141)
Colchicine	Transethosomal gel	Transdermal	Franz diffusion cell	Full-thickness rat skin	Nanoparticles are applied directly onto the skin	Phosphate buffer solution pH 6.4	37 ± 0.1°C/ 500 rpm	(142)
Diflunisal–phospholipid complex	Supramolecular nano-engineered lipid carrier	Transdermal	Franz diffusion cell	Full-thickness rat skin	Nanoparticles are applied directly onto the skin	Phosphate buffered saline pH 7.4	32 ± 0.5°C/NI	(143)
Indomethacin	Polymeric nanoparticles	Transdermal	Franz diffusion cell	Full-thickness rat skin	Nanoparticles are applied directly onto the skin	Phosphate buffered saline	32°C/NI	(144)
Lacidipine	Niosomal gel	Transdermal	Franz diffusion cell	Full-thickness rat skin	Nanoparticles are applied directly onto the skin	Ethanolic phosphate buffered saline pH 7.4 (30:70)	32 ± 2°C/ 200 rpm	(145)

Table III. (continued)

Drug type	Carrier system	Route	*In vitro* drug permeation method					Reference
			Method	Skin type	Application mode of nanocarrier	Permeation medium composition	Temperature/ agitation speed	
L-DOPA and carbidopa	Self-assembling nanomicellar system	Transdermal	Franz diffusion cell	Full-thickness rat and porcine skin	Nanoparticles are applied directly onto the skin	Phosphate buffered saline pH 7.4	37°C/NI	(146)
Pregabalin	Nanobased carrier	Transdermal	Franz diffusion cell	Full-thickness rat skin	Nanoparticles are applied directly onto the skin	Phosphate buffer solution pH 7.4	37 ± 0.5°C/NI	(147)
5-Fluorouracil	Nanogel	Topical	Vertical Franz diffusion cell	Full-thickness porcine ear skin	Nanogel dispersion is placed on the stratum corneum side of the skin	Phosphate buffer pH 4.5	32°C/NI	(49)
Acitretin and aloe emodin	Nanogel	Topical	Vertical Franz diffusion cell	Porcine ear skin	Nanogel pellets are dispersed in phosphate buffered saline pH 5.5 prior to application onto the skin	Acitretin:mixture of phosphate buffered saline pH 5.5 and methanol (7:3) Aloe emodin: phosphate buffered saline pH 5.5	32°C/NI	(57)
Quercetin	Solid lipid nanoparticle	Topical	Vertical Franz diffusion cell	Full-thickness human skin	Solid lipid nanoparticle formulation is applied onto the skin surface in donor compartment and occluded with Parafilm® to prevent evaporation	Phosphate buffer saline pH 7.4 with 1% Tween 20	37 ± 0.1°C/ 600 rpm	(103)
Ibuprofen sodium and indomethacin	Nanostructured supramolecular hydrogel	Topical	Vertical Franz diffusion cell	Abdominal human skin	Formulation is applied on donor compartment in contact with the epidermal side of the skin	Ibuprofen:phosphate buffer solution (pH 7.4, 10 nM) Indomethacin:ethanol	32°C/NI	(89)
Isotretinoin	Solid lipid nanoparticle	Topical	Vertical diffusion cell	Full-thickness abdominal rat skin	Isotretinoin-loaded solid lipid nanoparticles are gently placed on the skin membrane in donor chamber	Mixture of physiological saline and 95% ethanol (7:3)	37°C/ 300 rpm	(148)
Dipotassium glycyrrhizinate	Liposome	Topical	Vertical Franz diffusion cell	Full-thickness pig ear skin	Formulations are applied onto the skin surface	0.002% *w/v* aqueous sodium azide	37°C/NI	(149)
Octyl methoxycinnamate (OMC) and Nile red	Nanoparticle	Topical	Vertical Franz diffusion cell	Full-thickness porcine ear skin	Donor compartment consisting of skin membrane is filled with OMC carrier systems	Phosphate buffer solution with 5% *v/v* Tween 80	37 ± 2°C/ 200 rpm	(150)
Daidzein	Nanostructured lipid carrier	Transdermal	Vertical Franz diffusion cell	Full-thickness rat skin	Nanoparticles are applied directly onto the skin	Phosphate buffered saline pH 7.4 containing 20% ethanol	37 ± 0.5°C/ 300 rpm	(68)
Diclofenac diethyl amine	Polymeric nanoparticles	Transdermal		Full-thickness porcine skin	Nanoparticles are suspended in phosphate	Phosphate buffer solution pH 7.4	37°C/ 400 rpm	(70)

Table III. (continued)

Drug type	Carrier system	Route	*In vitro* drug permeation method					Reference
			Method	Skin type	Application mode of nanocarrier	Permeation medium composition	Temperature/ agitation speed	
			Vertical Franz diffusion cell		buffer solution pH 7.4 prior to the application onto the skin			
Ondansetron	Nanovesicular	Transdermal	Vertical Franz diffusion cell	Full-thickness rat skin	Nanoparticles are applied directly onto the skin	Phosphate buffer solution pH 7.4	32 °C / 100 rpm	(151)
Diclofenac acid	Nanosuspension	Transdermal	Vertical Franz diffusion cell	Full-thickness porcine skin	Nanoparticles are applied directly onto the skin	Saline solution	37 ± 1°C/NI	(152)
Eprosartan mesylate	Nanovesicles	Transdermal	Vertical Franz diffusion cell	Full-thickness rat skin	Nanoparticles are applied directly onto the skin	Ethanolic phosphate buffered saline pH 7.4 (20:80)	37 °C / 100 rpm	(153)
Meloxicam	Flexosomes (flexible liposomes)	Transdermal	Vertical Franz diffusion cell	Full-thickness rat skin	Nanoparticles are applied directly onto the skin	Phosphate buffer solution pH 7.4 containing 5% Tween 8	37°C/NI	(154)
Risperidone	Nanosoft lipid vesicle	Transdermal	Transdermal diffusion cell	Full-thickness rat skin	Nanoparticles are applied directly onto the skin	Ethanol:phosphate buffer solution (3:7)	NI	(155)
Vitamin A	Solid lipid nanoparticles	Topical	K – C diffusion cell	Abdominal human cadaver skin	A gel containing vitamin A-loaded solid lipid nanoparticles is directly applied onto the skin surface	Phosphate buffer saline with 3% polysorbate 80	NI	(78)
Amphotericin B	Solid lipid nanoparticles	Topical	K – C diffusion cell	Full-thickness abdominal rat skin	Solid lipid nanoparticle formulations are placed on the skin membrane in the donor chamber	Mixture of physiological buffer solution pH 6.8 and methanol (7:3)	32 ± 0.5 °C/ 300 rpm	(156)
Osthole	Nanovesicles	Transdermal	Side-by-side diffusion cell	Full-thickness porcine skin	Nanoparticles are applied directly onto the skin	20% ethanol solution	32 ± 0.5 °C/ 100 rpm	(157)
Paeonol	Transethosomes	Transdermal	Valia-Chien chamber (horizontal diffusion cell)	Full-thickness porcine skin	Nanoparticles are applied directly onto the skin	20% ethanol solution	32 °C / 100 rpm	(158)

NI = not indicated

moisture loss from the sample. The aliquots are withdrawn from the receiving chamber and subjected to drug assay using analytical techniques similar to dissolution tests of topical nanocarriers.

Microcentrifuge Tube

The release rate of clonidine from nanoparticles has been determined using a microcentrifuge tube system (102). Phosphate buffered saline pH 7.4 with 0.1% sodium azide and 0.1% Tween 80 is used as the dissolution medium. The dissolution temperature is kept at 37°C. The suspended nanoparticles in the dissolution medium are subjected to vortex with drug dissolution determined by means of the liquid-scintillation counting technique.

In Situ Fiber Optic Probe Dissolution Apparatus

The modern automated fiber optic probe dissolution apparatus allows the *in situ* measurement of dissolved drug directly in the dissolution vessel by the fiber optic probe system. The probes are available in a variety of shapes, sizes, orientations (placing through the vessel cover or on a manifold), and designs (arch, in shaft, in resident, in resident but partially out during sampling). The system essentially transmits the light from a spectrophotometer (UV–visible/photodiode array spectrophotometers) to a dissolution vessel, and then the light is returned to the spectrophotometer where the absorbance of analyte is measured (112,113) (Fig. 9). This setup real-time monitors the drug dissolution profile and provides instant information on the product performance. Undissolved particles (excipients) from a dosage form may induce spectrophotometric interference by blocking light transmission, which shines through the sample for measurement. The absorbance incurred by excipients may be added to the absorbance of the dissolved analyte during the real-time sample analysis (115). Skin and powder-based products with no excipients to interfere with the analysis as well as modified parenteral products (nanospheres and liposomes) may be more appropriate to be characterized using this apparatus.

The fiber optic probe system is applicable to the analysis of both immediate- and controlled-release formulations (113,116). Bijlani *et al*. (117) monitor the fraction of drug released from immediate- and prolonged-release microparticulate spheroids containing ibuprofen. The dissolution profiles obtained by the fiber optic probe system are more accurate with lower and consistent standard deviations particularly for immediate-release multiparticulates, faster in operation, and less labor intensive when compared to the high-performance liquid chromatography method. Voisine *et al*. (118) test the *in vitro* release of cefazolin from poly(lactic-co-glycolic) acid microspheres using USP apparatus 2 and 4 coupled with *in situ* UV fiber optic probe. The use of USP apparatus 2 coupled with *in situ* UV fiber optic probe is found to have microspheres accumulated at the probe and interfere with the probe detection window. Liu *et al*. (119) measure 24-h drug release from extended-release tablets containing compound A using *in situ* fiber optics dissolution method and conclude that the method is simple and convenient for producing precise, accurate, reproducible, and robust dissolution data. Till today, none of the skin nanoproducts are characterized using a fiber optic probe system with respect to drug dissolution.

DRUG PERMEATION METHODS FOR NANOCARRIERS

The availability of drugs in the epidermis and dermis as well as in systemic circulation is essential for the treatment or prevention of localized and systemic diseases, respectively (120). The drug availability is brought about by penetration of dissolved drug from the skin surfaces or nanocarriers bringing the drug load into the skin tissues and/or blood (121,122). The skin drug/nanocarrier penetration leads to drug retention in skin tissues and/or permeation in the bloodstream. The topical nanocarriers are designed to deliver drugs into the skin tissues, whereas the transdermal nanocarriers are primarily designated to introduce the drugs in the systemic circulation. The characterization of drug permeation profiles of transdermal carriers is imperative to enable one to understand the drug pharmacokinetics and pharmacodynamics properties. The same characterization may be conducted with reference to topical nanocarriers to profile local as well as systemic drug levels. The latter is indeed critical when local therapy is advocated to minimize the systemic adverse effects of therapeutics such as anticancer drugs.

The local drug retention in the skin is commonly examined by chemical or radiation assay of skin treated with nanocarriers, with Fourier transform infrared imaging being employed in recent years (86). The drug permeation profiles of topical and transdermal nanocarriers are evaluated using similar methods as drug dissolution tests. The major difference lies in the replacement of synthetic membrane with skin tissue (full-thickness skin, epidermis, or stratum corneum) from rat, mice, pig, goat, and human (82). Table III summarizes the types of drugs and nanocarriers and permeation test parameters in association with skin dosage forms. Porcine abdominal skin is highly preferred as the model membrane for drug permeation study because of its similarity to human skin in terms of skin layer thickness, morphology (follicular structure, vascular anatomy, and arrangement of dermal collagen fibers), contents of glycosphingolipids and ceramides, and permeability of drugs compared to several other animal species (49,123–125,159–165). The thickness of the model skin plays a major role in the drug permeation study (124). Full-thickness skin may not be physiologically relevant as a barrier to the diffusion of lipophilic drugs. Split thickness or strongly dermatomed skin is recommended for permeation studies of lipophilic drugs (166). However, the shortcomings observed with thin skin samples are the irregular and inconsistent increase in drug fluxes over time. The small aberrations that occurred during dermatomation of the skin to thin layers may be attributed to variation of results. It is suggested that a compromise on suitable skin thickness is needed where homogeneous skin samples devoid of any aberrations and without creating an unphysiologically strong barrier for water-insoluble drugs is required.

The composition of a receptor medium must be innocuous to the skin (82). Ethanol has been shown to increase skin drug permeation in comparison to ethanol-free buffer (124). The ethanol is deemed to be able to extract the skin lipids thus facilitating skin drug permeation and giving rise to artifacts in drug permeation evaluation. Nonionic surfactants are reported to incur less changes to the physicochemical states of the skin and influence the process of skin drug permeation minimally (167). The receptor medium must be available in sink condition where its drug concentration should not be more than 10% of drug saturation to avoid receptor fluid acting as a rate-limiting step in skin drug permeation (168–170). Typically, physiological saline or phosphate buffer is used as a receptor medium. Current OECD guidelines recommend normal saline as a receptor medium for hydrophilic compounds and mixture of normal saline and nonionic surfactants (Tween 80) or other solvents such as ethanol and water (50% aqueous ethanol solution), polyoxyethelene (20), oleyl ether (< 6%) in water, or 5% bovine serum albumin for lipophilic compounds in skin permeation studies with Franz diffusion cells (170–172). The incorporation of additives in the receptor medium is a prerequisite in some cases to increase the drug's solubility. However, these additives should not alter the integrity of the model skin and drug permeability rate. To prevent microbiological growth in the receptor medium, preservatives such as gentamicin, sodium azide (0.02 to 0.05%), and formaldehyde (0.1%) may be added (82). Overall, pure phosphate buffer represents the receptor medium of choice on the note that undesired interactions with skin constituents or dosage forms can be avoided.

Different from *in vitro* drug dissolution study, the drug permeation tests of skin nanocarriers use biological tissue as the model membrane. The skin tissue needs to be thawed and hydrated by the receptor medium prior to skin drug permeation analysis (123,148). The epidermis or stratum corneum of the skin tissue must face the donor compartment, and the dermis or lower surface of epidermis or stratum corneum must face the receptor compartment (173). Klang *et al.* (124) conduct comparative experiments with occluded condition of the donor compartment and sampling arm to prevent evaporation and nonoccluded condition with an open donor compartment. Skin drug permeation with large standard deviations is attained when nonoccluded conditions are adopted in all the drug doses applied (5, 50, and 500 mg/cm^2). In another study by Bose *et al.* (103), the use of occluded donor compartment of vertical Franz diffusion cell prevents full-thickness human skin from moisture loss by evaporation. A higher skin drug retention is observed against the case of using the nonoccluded donor compartment, due to increased hydration of the stratum corneum under occluded conditions.

BRIEF COMMENTS ON *IN VITRO–IN VIVO* CORRELATION OF NANOSIZED DOSAGE FORMS

In vitro–in vivo correlation (IVIVC) is a predictive mathematical approach describing the relationship between *in vitro* drug dissolution (drug release profile) and *in vivo* performance (plasma concentration–time profile) of the same dosage form (174). An overestimation and underestimation of product dissolution profiles using nonstandard *in vitro* methods result in an inaccurate prediction of *in vivo* performance and lead to failure in clinical trials (175). As described by the USFDA, there are four levels of IVIVC which include level A (*in vitro* dissolution *vs. in vivo* absorption), level B (*in vitro* mean dissolution time *vs. in vivo* mean residence time or mean absorption time), level C (*in vitro* $T_{50\%}$ *vs. in vivo* T_{max}), and multiple level C (relationship between one or more pharmacokinetic parameters, *i.e.*, C_{max}, T_{max}, or AUC, and amount dissolved at several time points, *i.e.*, at least 3 dissolution time points at early, middle, and late stages of dissolution profile). Among the four, level A and multiple level C correlations are considered the useful and most informative. Level A IVIVC is preferred and recommended as it represents a point-to-point relationship between *in vitro* dissolution rate and *in vivo* absorption rate of the drug from a dosage form compared to correlation of a few time points in multiple level C. This allows a thorough *in vivo* prediction of dosage form which accelerates the drug development process and also assists in regulatory agency approvals (176). Level B and level C are limited in predicting *in vivo* performance of a drug product as level B is not a point-to-point correlation and level C is a single-point analysis. Developing a standard *in vitro* dissolution test that accurately correlates the *in vivo* product performance not only augments the utility of an *in vitro* study but also serves as a good quality control tool as an indicator of *in vivo* performance (177). The literature survey reveals that IVIVC has been performed for several oral-based nanosized preparations using animal models such as indomethacin gelatin nanoparticles (178), silybin meglumine silica nanoparticles (179), simvastatin nanostructure lipid carriers (180), and fenofibrate nanosuspension (181). It has been performed for conventional transdermal delivery systems of drugs but not in the form of nanosized dosage forms, *i.e.*, estradiol drug in adhesive (182), lidocaine patch (183), and pentoxifylline gel (184). Despite IVIVC having a great value in the development of biopharmaceuticals, to the best of our knowledge, no reports on IVIVC with respect to topical and transdermal-based nanosized dosage forms have been found and no regulatory IVIVC guidance is available for complex nonoral drug products. The major challenge to develop IVIVC for topical/transdermal novel dosage forms is complexity of drug release/penetration/permeation mechanisms. The present recommended compendial *in vitro* dissolution apparatus for skin drug products such as the paddle over disk/disk assembly method (USP apparatus 5), rotating cylinder (USP apparatus 6), reciprocating disk (USP apparatus 7), and paddle over extraction cell method may not reflect accurately the complex mechanisms of penetration/permeation/diffusion of nanocarriers across the skin (185). It is necessary to focus on a suitable IVIVC model that can precisely correlate the *in vitro* and *in vivo* data during the development of topical and transdermal nanodrug delivery systems in order to maximize the development and commercialization potential of nanosized formulations through reducing the drug development timeframe and cost. Through examining the current status of *in vitro* drug dissolution and permeation tests of skin nanocarrier systems, one realizes that there is no appropriate and robust biorelevant *in vitro* method for successful IVIVC; at least efforts to identify one have yet to be demonstrated.

The main hurdle is the challenges associated with accurate characterization of penetration, retention, and permeation profiles of drugs *in vivo*.

CHALLENGES AND FUTURE PROSPECTIVE

Over the past few decades, an extensive level of research activities has taken place with the aim to achieve breakthroughs in topical and transdermal delivery of various pharmaceutical actives through the advancement of nanotechnology. Nevertheless, several challenges have yet to be addressed. Currently, only a few of USFDA-approved *in vitro* dissolution methods are available for conventional topical/transdermal drug products and a few other methods are developed as a part of research activities. The present regulatory guidelines offer partially standardized methods such as Franz diffusion cell for *in vitro* skin permeation studies using human/cadaver/animal skin as the biological membrane. This leads to researchers exploring and utilizing various experimental protocols in terms of equipment design, nature of the dissolution medium, nature of the membrane, sampling intervals, temperature, and rotational speed. These experimental setups lack validation against *in vitro* dissolution and *in vitro* skin penetration/permeation correlation status. Their biorelevance with reference to *in vivo* plasma concentration–time profiles (IVIVC) is not known. Such gaps render the interrelation of various *in vitro* studies being not comparable and the translation of *in vitro* data for *in vivo* or clinical performance prediction impossible. Future focus should emphasize on fully validated improved versions of existing *in vitro* testing methods and development of new technologies like automated fiber optic probe-based dissolution system combined with spectroscopy for standardized *in vitro* dissolution and permeation testing of topical/transdermal-based formulations containing nanomaterials with accurate, precise, and reliable data which are biorelevant and contributive to IVIVC.

COMPLIANCE WITH ETHICAL STANDARDS

Conflict of Interest The authors declare that they have no conflict of interest.

REFERENCES

1. Hamblin M, Avci P, Prow T. Nanoscience in dermatology. 1st ed. Cambridge: Academic; 2016.
2. Abla MJ, Singh ND, Banga AK. Role of nanotechnology in skin delivery of drugs. In: Dragicevic N, Maibach H, editors. Percutaneous penetration enhancers chemical methods in penetration enhancement: nanocarriers. Berlin: Springer; 2016. p. 1–10.
3. Caster JM, Patel AN, Zhang T, Wang A. Investigational nanomedicines in 2016: a review of nanotherapeutics currently undergoing clinical trials. Interdiscip Rev Nanomed Nanobiotechnol. 2017;9(1):e1416. https://doi.org/10.1002/wnan.1416.
4. Williams AC. Transdermal and topical drug delivery. From theory to clinical practice. London: Pharmaceutical Press; 2003.
5. Ye C, Qiu H, Seixas MDG, Bazin R, Flament F, Cointereau-Chardon S, *et al*. Facial skin pores: a multiethnic study. Clin Cosmet Investig Dermatol. 2015;8:85. https://doi.org/10.2147/ccid.s74401.
6. Otberg N, Richter H, Schaefer H, Blume-Peytavi U, Sterry W, Lademann J. Variations of hair follicle size and distribution in different body sites. J Invest Dermatol. 2004;122(1):14–9. https://doi.org/10.1046/j.0022-202X.2003.22110.x.
7. Luengo J, Lehr C-M, Otberg N, Teichmann A, Blume-Peytavi U, Richter H, *et al*. Nanoparticles—an efficient carrier for drug delivery into the hair follicles. Eur J Pharm Biopharm. 2006;66(2):159–64. https://doi.org/10.1016/j.ejpb.2006.10.019.
8. Patzelt A, Mak WC, Jung S, Knorr F, Meinke MC, Richter H, *et al*. Do nanoparticles have a future in dermal drug delivery? J Control Release. 2017;246:174–82. https://doi.org/10.1016/j.jconrel.2016.09.015.
9. Nastiti CMRR, Ponto T, Abd E, Grice JE, Benson HAE, Roberts MS. Topical nano and microemulsions for skin delivery. Pharmaceutics. 2017;9(4):37. https://doi.org/10.3390/pharmaceutics9040037.
10. Delouise LA. Applications of nanotechnology in dermatology. J Invest Dermatol. 2012;132(3 PART 2):964–75. https://doi.org/10.1038/jid.2011.425.
11. Ng K, Lau W. Skin deep: the basics of human skin structure and drug penetration. In: Dragicevic N, Maibach H, editors. Percutaneous penetration enhancers chemical methods in penetration enhancement: drug manipulation strategies and vehicle effects. Berlin: Springer; 2015. p. 3–10. https://doi.org/10.1007/978-3-662-45013-0.
12. Baroli B. Penetration of nanoparticles and nanomaterials in the skin: fiction or reality? J Pharm Sci. 2010;99(1):21–50. https://doi.org/10.1002/jps.21817.
13. Grice JE, Moghimi HR, Ryan E, Zhang Q, Haridass I, Mohammed Y, *et al*. Non-formulation parameters that affect penetrant-skin-vehicle interactions and percutaneous absorption. In: Dragicevic N, Maibach H, editors. Percutaneous penetration enhancers drug penetration into/through the skin: methodology and general considerations. Berlin: Springer; 2017. p. 45–75. https://doi.org/10.1007/978-3-662-53270-6.
14. Surber C, Humbert P, Abels C, Maibach H. The acid mantle: a myth or an essential part of skin health? Curr Probl Dermatol. 2018;54:1–10. https://doi.org/10.1159/000489512.
15. Elias PM. Stratum corneum defensive functions: an integrated view. J Invest Dermatol. 2005;125(2):183–200. https://doi.org/10.1111/j.0022-202X.2005.23668.x.
16. Schmid-Wendtner MH, Korting HC. The pH of the skin surface and its impact on the barrier function. Skin Pharmacol Physiol. 2006;19(6):296–302. https://doi.org/10.1159/000094670.
17. Grice EA, Segre JA. The skin microbiome. Nat Rev Microbiol. 2011;9(4):244–53. https://doi.org/10.1038/nrmicro2537.
18. US Food and Drug Administration. Guidance for industry considering whether an FDA-regulated product involves the application of nanotechnology. 2014.
19. Rivera Gil P, Hühn D, del Mercato LL, Sasse D, Parak WJ. Nanopharmacy: inorganic nanoscale devices as vectors and active compounds. Pharmacol Res. 2010;62(2):115–25. https://doi.org/10.1016/j.phrs.2010.01.009.
20. Harjoh N, Wong T, Nawaz A, Khan N, Harun M. Nanocarriers and their actions to improve skin permeability and transdermal drug delivery. Curr Pharm Des. 2015;21(20):2848–66. https://doi.org/10.2174/1381612821666150428145216.
21. Chityal G, Poornachandra Y, Pombala S. Therapeutic nanomaterials: from a drug delivery perspective. In: Andronescu E, Grumezescu A, editors. Nanostructures for drug delivery. Amasterdam: Elsevier; 2017. p. 1–61.
22. Pardeike J, Hommoss A, Müller RH. Lipid nanoparticles (SLN, NLC) in cosmetic and pharmaceutical dermal products. Int J Pharm. 2009;366(1–2):170–84. https://doi.org/10.1016/j.ijpharm.2008.10.003.
23. Contri R, Fiel L, Pohlmann A, Guterres S, Beck R. Transport of substances and nanoparticles across the skin and in vitro models to evaluate skin permeation and/or penetration. In:

Beck R, Guterres S, Pohlmann A, editors. Nanocosmetics and nanomedicines. Berlin: Springer; 2011. p. 3–36. https://doi.org/10.1007/978-3-642-19792-5.
24. Neubert RHH. Potentials of new nanocarriers for dermal and transdermal drug delivery. Eur J Pharm Biopharm. 2011;77(1):1–2. https://doi.org/10.1016/j.ejpb.2010.11.003.
25. Palmer BC, DeLouise LA. Nanoparticle-enabled transdermal drug delivery systems for enhanced dose control and tissue targeting. Molecules. 2016;21(12):1719. https://doi.org/10.3390/molecules21121719.
26. Vogt A, Lendlein A, Alexiev U, Neffe AT, Wischke C, Ma N. Nanocarriers for drug delivery into and through the skin—do existing technologies match clinical challenges? J Control Release. 2016;242:3–15. https://doi.org/10.1016/j.jconrel.2016.07.027.
27. Bibi N, Ahmed N, Khan G. Nanostructures in transdermal drug delivery systems. In: Andronescu E, Grumezescu A, editors. Nanostructures for drug delivery. Amsterdam: Elsevier; 2017. p. 639–68.
28. Bhatia S. Natural polymer drug delivery systems: nanoparticles, plants, and algae. Cham: Springer International Publishing; 2016.
29. Mura S, Nicolas J, Couvreur P. Stimuli-responsive nanocarriers for drug delivery. Nat Mater. 2013;12(11):991–1003. https://doi.org/10.1038/nmat3776.
30. D'Mello SR, Chen M-L, Lee SL, Cruz CN, Tyner KM, Kapoor M. The evolving landscape of drug products containing nanomaterials in the United States. Nat Nanotechnol. 2017;12(6):523–9. https://doi.org/10.1038/nnano.2017.67.
31. Abu Samah N, Heard C. The effects of topically applied polyNIPAM-based nanogels and their monomers on skin cyclooxygenase expression, ex vivo. Nanotoxicology. 2014;8(1):100–6. https://doi.org/10.3109/17435390.2012.754511.
32. Selzer D, Schaefer UF, Lehr CM, Hansen S. Basic mathematics in skin absorption. In: Dragicevic N, Maibach H, editors. Percutaneous penetration enhancers drug penetration into/through the skin: methodology and general considerations. Berlin: Springer; 2017. p. 3–25. https://doi.org/10.1007/978-3-662-53270-6_1.
33. Shah V, Skelly J. In vitro methodology: practical considerations in developing a quality control (in vitro release) procedure for topical drug products. In: Shah V, Maibach H, editors. Topical drug bioavailability, bioequivalence, and penetration. Boston: Springer; 1993. p. 107–16. https://doi.org/10.1007/978-1-4899-1262-6.
34. Dizaj S, Vazifehasl Z, Salatin S, Adibkia K, Javadzadeh Y. Nanosizing of drugs: effect on dissolution rate. Research in pharmaceutical sciences. Res Pharm Sci. 2015 [2019 Feb 28];10(2):95–108.
35. US Food and Drug Administration. Guidance for industry: drug products, including biological products, that contain nanomaterials. 2017.
36. Scheubel E. Predictive in vitro dissolution tools: application during formulation development. Clermont-Ferrand: Université d'Auvergne Clermont-Ferrand I; 2010.
37. Marques M, Ueda CT, Shah VP, Derdzinski K, Ewing G, Flynn G, *et al*. Topical and transdermal drug products. Pharmacopeial Forum. 2009;35(3):750–64.
38. Brown CK, Friedel HD, Barker AR, Buhse LF, Keitel S, Cecil TL, *et al*. FIP/AAPS joint workshop report: dissolution/in vitro release testing of novel/special dosage forms. Dissolut Technol. 2011;18(4):51–64. https://doi.org/10.1208/s12249-011-9634-x.
39. Chang R-K, Raw A, Lionberger R, Yu L. Generic development of topical dermatologic products: formulation development, process development, and testing of topical dermatologic products. AAPS J. 2013;15(1):41–52. https://doi.org/10.1208/s12248-012-9411-0.
40. Mansour H, Park C-W. Therapeutic applications and targeted delivery of nanomedicines and nanopharmaceutical products. In: Brenner S, editor. The clinical nanomedicine handbook. Boca Raton: CRC; 2013. p. 321–34.
41. Tinkle S, Mcneil SE, Mühlebach S, Bawa R, Borchard G, Barenholz YC, *et al*. Nanomedicines: addressing the scientific and regulatory gap. Ann N Y Acad Sci. 2014;1313(1):35–56. https://doi.org/10.1111/nyas.12403.
42. Weissig V, Pettinger T, Murdock N. Nanopharmaceuticals (part 1): products on the market. Int J Nanomedicine. 2014;9(1):4357–73. https://doi.org/10.2147/IJN.S46900.
43. Tadicherla S, Berman B. Percutaneous dermal drug delivery for local pain control. Ther Clin Risk Manag. 2006;2(1):99–113.
44. Praca F, Campos P, Eloy J, Petrilli R, Bentley M, Medina W. Topical photodynamic therapy for skin diseases: current status of preclinical and clinical research, nanocarriers and physical methods for photosensitizer delivery. In: Ascenso A, Simões S, Ribeiro H, editors. Carrier-mediated dermal delivery: applications in the prevention and treatment of skin disorders. Singapore: Pan Stanford; 2017.
45. Siewert M, Dressman J, Brown CK, Shah VP, Aiache J-M, Aoyagi N, *et al*. FIP/AAPS guidelines to dissolution/in vitro release testing of novel/special dosage forms. AAPS PharmSciTech. 2003;4(1):43–52. https://doi.org/10.1208/pt040107.
46. Copley T. Performance testing for topical and transdermal drug delivery. Am Pharm Rev. 2016:1–7.
47. D'Souza S. A review of in vitro drug release test methods for nano-sized dosage forms. Adv Pharm. 2014;2014:1–12. https://doi.org/10.1155/2014/304757.
48. Shen J, Burgess DJ. In vitro dissolution testing strategies for nanoparticulate drug delivery systems: recent developments and challenges. Drug Deliv Transl Res. 2013;3(5):409–15. https://doi.org/10.1007/s13346-013-0129-z.
49. Sabitha M, Sanoj R, Nair A, Lakshmanan V-K, Nair SV, Jayakumar R. Development and evaluation of 5-fluorouracil loaded chitin nanogels for treatment of skin cancer. Carbohydr Polym. 2013;91(1):48–57. https://doi.org/10.1016/J.CARBPOL.2012.07.060.
50. Khalil SKH, El-Feky GS, El-Banna ST, Khalil WA. Preparation and evaluation of warfarin-β-cyclodextrin loaded chitosan nanoparticles for transdermal delivery. Carbohydr Polym. 2012;90(3):1244–53. https://doi.org/10.1016/j.carbpol.2012.06.056.
51. Liu Y, Nguyen A, Allen A, Zoldan J, Huang Y, Chen JY. Regenerated cellulose micro-nano fiber matrices for transdermal drug release. Mater Sci Eng C. 2017;74:485–92. https://doi.org/10.1016/J.MSEC.2016.12.048.
52. Elmowafy M, Samy A, Abdelaziz AE, Shalaby K, Abdelgawad MA, Raslan MA, *et al*. Polymeric nanoparticles based topical gel of poorly soluble drug: formulation, ex-vivo and in vivo evaluation. Beni-Suef Univ J Basic Appl Sci. 2017;6(2):184–91. https://doi.org/10.1016/j.bjbas.2017.03.004.
53. Jug M, Hafner A, Lovrić J, Kregar ML, Pepić I, Vanić Ž, *et al*. An overview of in vitro dissolution/release methods for novel mucosal drug delivery systems. J Pharm Biomed Anal. 2018;147:350–66. https://doi.org/10.1016/j.jpba.2017.06.072.
54. Kelidari HR, Saeedi M, Akbari J, Morteza-Semnani K, Gill P, Valizadeh H, *et al*. Formulation optimization and in vitro skin penetration of spironolactone loaded solid lipid nanoparticles. Colloids Surf B Biointerfaces. 2015;128:473–9. https://doi.org/10.1016/j.colsurfb.2015.02.046.
55. Moazeni M, Kelidari HR, Saeedi M, Morteza-Semnani K, Nabili M, Gohar AA, *et al*. Time to overcome fluconazole resistant Candida isolates: solid lipid nanoparticles as a novel antifungal drug delivery system. Colloids Surf B Biointerfaces. 2016;142:400–7. https://doi.org/10.1016/j.colsurfb.2016.03.013.
56. Somagoni J, Patel AR, Boakye CHA, Singh M, Zucolotto V, Mendonca Faria HA, *et al*. Nanomiemgel—a novel drug delivery system for topical application—in vitro and in vivo evaluation. PLoS One. 2014;9(12):e115952. https://doi.org/10.1371/journal.pone.0115952.
57. Gupta S, Jayakumar R, Panonnummal R, Sabitha M, Divya G. Acitretin and aloe-emodin loaded chitin nanogel for the treatment of psoriasis. Eur J Pharm Biopharm. 2016;107:97–109. https://doi.org/10.1016/j.ejpb.2016.06.019.
58. Panonnummal R, Jayakumar R, Sabitha M. Comparative antipsoriatic efficacy studies of clobetasol loaded chitin nanogel and marketed cream. Eur J Pharm Sci. 2017;96:193–206. https://doi.org/10.1016/j.ejps.2016.09.007.
59. Kaur A, Katiyar SS, Kushwah V, Jain S. Nanoemulsion loaded gel for topical co-delivery of clobitasol propionate and calcipotriol in psoriasis. Nanomedicine. 2017;13(4):1473–82. https://doi.org/10.1016/j.nano.2017.02.009.

60. Hua S. Comparison of in vitro dialysis release methods of loperamide-encapsulated liposomal gel for topical drug delivery. Int J Nanomedicine. 2014;9(1):735–44. https://doi.org/10.2147/IJN.S55805.
61. Noshi SH. Lipid-based drug delivery systems for the enhancement of topical delivery of benzocaine. J Pharm Biol Sci. 2018;13(3):13–9. https://doi.org/10.9790/3008-1303011319.
62. Hussain A, Samad A, Nazish I, Ahmed FJ. Nanocarrier-based topical drug delivery for an antifungal drug. Drug Dev Ind Pharm. 2014;40(4):527–41. https://doi.org/10.3109/03639045.2013.771647.
63. Sanap GS, Mohanta GP. Development of miconazole nitrate controlled release formulations based on SLN and NLC for topical delivery. Int J Pharm Pharm Sci. 2014;6(4):393–9.
64. Yang M, Gu Y, Yang D, Tang X, Liu J. Development of triptolide-nanoemulsion gels for percutaneous administration: physicochemical, transport, pharmacokinetic and pharmacodynamic characteristics. J Nanobiotechnology. 2017;15(1):88. https://doi.org/10.1186/s12951-017-0323-0.
65. Deva P. Nanoparticulate drug delivery systems, in vitro drug release test methods. Int J Pharma Bio Sci. 2017;8(3):103–19. https://doi.org/10.22376/ijpbs.2017.8.3.p103-119.
66. Jana S, Manna S, Nayak AK, Sen KK, Basu SK. Carbopol gel containing chitosan-egg albumin nanoparticles for transdermal aceclofenac delivery. Colloids Surf B Biointerfaces. 2014;114:36–44. https://doi.org/10.1016/j.colsurfb.2013.09.045.
67. Chen H, Wang Y, Zhai Y, Zhai G, Wang Z, Liu J. Development of a ropivacaine-loaded nanostructured lipid carrier formulation for transdermal delivery. Colloids Surf A Physicochem Eng Asp. 2015;465(465):130–6. https://doi.org/10.1016/j.colsurfa.2014.10.046.
68. Song J, Fan X, Shen Q. Daidzein-loaded nanostructured lipid carriers-PLGA nanofibers for transdermal delivery. Int J Pharm. 2016;501(1–2):245–52. https://doi.org/10.1016/j.ijpharm.2016.02.003.
69. Elgindy NA, Mehanna MM, Mohyeldin SM. Self-assembled nano-architecture liquid crystalline particles as a promising carrier for progesterone transdermal delivery. Int J Pharm. 2016;501(1–2):167–79. https://doi.org/10.1016/j.ijpharm.2016.01.049.
70. Dias SFL, Nogueira SS, De França DF, Guimarães MA, De Oliveira Pitombeira NA, Gobbo GG, *et al*. Acetylated cashew gum-based nanoparticles for transdermal delivery of diclofenac diethyl amine. Carbohydr Polym. 2016;143:254–61. https://doi.org/10.1016/j.carbpol.2016.02.004.
71. Ahmad A, Abuzinadah MF, Alkreathy HM, Banaganapalli B, Mujeeb M. Ursolic acid rich *Ocimum sanctum* L leaf extract loaded nanostructured lipid carriers ameliorate adjuvant induced arthritis in rats by inhibition of COX-1, COX-2, TNF-α and IL-1: pharmacological and docking studies. Davis KR, editor. PLoS One. 2018;13(3):e0193451. https://doi.org/10.1371/journal.pone.0193451.
72. Singh I, Saraf SA, Singh S, Saha S, Parashar P, Kanoujia J. Transdermal potential and anti-gout efficacy of febuxostat from niosomal gel. J Drug Deliv Sci Technol. 2017;39:348–61. https://doi.org/10.1016/j.jddst.2017.04.020.
73. Mohseni M, Ilka R, Mehravi B, Ashtari K, Abnoos M, Mousavi SAJ. Chitosan-alginate nano-carrier for transdermal delivery of pirfenidone in idiopathic pulmonary fibrosis. Int J Biol Macromol. 2018;118:1319–25. https://doi.org/10.1016/j.ijbiomac.2018.04.147.
74. Garg NK, Sharma G, Singh B, Nirbhavane P, Tyagi RK, Shukla R, *et al*. Quality by design (QbD)-enabled development of aceclofenac loaded-nano structured lipid carriers (NLCs): an improved dermatokinetic profile for inflammatory disorder(s). Int J Pharm. 2017;517(1–2):413–31. https://doi.org/10.1016/j.ijpharm.2016.12.010.
75. Elmataeeshy ME, Sokar MS, Bahey-El-Din M, Shaker DS. Enhanced transdermal permeability of terbinafine through novel nanoemulgel formulation; development, in vitro and in vivo characterization. Future J Pharm Sci. 2018;4(1):18–28. https://doi.org/10.1016/j.fjps.2017.07.003.
76. Vaghasiya H, Kumar A, Sawant K. Development of solid lipid nanoparticles based controlled release system for topical delivery of terbinafine hydrochloride. Eur J Pharm Sci. 2013;49(2):311–22. https://doi.org/10.1016/j.ejps.2013.03.013.
77. Domínguez-Villegas V, Clares-Naveros B, García-López ML, Calpena-Campmany AC, Bustos-Zagal P, Garduño-Ramírez ML. Development and characterization of two nano-structured systems for topical application of flavanones isolated from Eysenhardtia platycarpa. Colloids Surf B Biointerfaces. 2014;116:183–92. https://doi.org/10.1016/j.colsurfb.2013.12.009.
78. Pople P, Singh K. Development and evaluation of topical formulation containing solid lipid nanoparticles of vitamin A. AAPS PharmSciTech. 2006;7(4):91–E69. https://doi.org/10.1208/pt070491.
79. Ng SF, Rouse J, Sanderson D, Eccleston G. A comparative study of transmembrane diffusion and permeation of ibuprofen across synthetic membranes using Franz diffusion cells. Pharmaceutics. 2010;2(2):209–23. https://doi.org/10.3390/pharmaceutics2020209.
80. Singh S, Singh M, Tripathi CB, Arya M, Saraf SA. Development and evaluation of ultra-small nanostructured lipid carriers: novel topical delivery system for athlete's foot. Drug Deliv Transl Res. 2016;6(1):38–47. https://doi.org/10.1007/s13346-015-0263-x.
81. Teledyne Hanson Research. Vertical diffusion cell 6-cell manual diffusion test system. https://hansonresearch.com/diffusion-testing/manual-diffusion/. Accessed 14 Aug 2018.
82. de Lino MES, ALM R, Perissinato AG, Pereira GR, Mudrik PS. Evaluation of skin absorption of drugs from topical and transdermal formulations. Braz J Pharm Sci. 2016;52(3):527–44. https://doi.org/10.1590/s1984-82502016000300018.
83. Murthy SN, Hiremath SRR. Physical and chemical permeation enhancers in transdermal delivery of terbutaline sulphate. AAPS PharmSciTech. 2004;2(1):1–5. https://doi.org/10.1208/pt0201_tn1.
84. Fang JY, Fang CL, Liu CH, Su YH. Lipid nanoparticles as vehicles for topical psoralen delivery: solid lipid nanoparticles (SLN) versus nanostructured lipid carriers (NLC). Eur J Pharm Biopharm. 2008;70(2):633–40. https://doi.org/10.1016/j.ejpb.2008.05.008.
85. Calpena AC, Souto EB, Garduño-Ramirez ML, García ML, Clares B, Abrego G, *et al*. Nanoemulsions for dermal controlled release of oleanolic and ursolic acids: in vitro, ex vivo and in vivo characterization. Colloids Surf B Biointerfaces. 2015;130:40–7. https://doi.org/10.1016/j.colsurfb.2015.03.062.
86. Nawaz A, Wong TW. Chitosan-carboxymethyl-5-fluorouracil-folate conjugate particles: microwave modulated uptake by skin and melanoma cells. J Invest Dermatol. 2018;138(11):2412–22. https://doi.org/10.1016/j.jid.2018.04.037.
87. Khan NR, Wong TW. Microwave-aided skin drug penetration and retention of 5-fluorouracil-loaded ethosomes. Expert Opin Drug Deliv. 2016;13(9):1209–19. https://doi.org/10.1080/17425247.2016.1193152.
88. Khan NR, Wong TW. 5-Fluorouracil ethosomes—skin deposition and melanoma permeation synergism with microwave. Artif Cells Nanomed Biotechnol. 2018;46(sup1):568–77. https://doi.org/10.1080/21691401.2018.1431650.
89. Limón D, Amirthalingam E, Rodrigues M, Halbaut L, Andrade B, Garduño-Ramírez ML, *et al*. Novel nanostructured supramolecular hydrogels for the topical delivery of anionic drugs. Eur J Pharm Biopharm. 2015;96:421–36. https://doi.org/10.1016/j.ejpb.2015.09.007.
90. Al-Kassas R, Wen J, Cheng AEM, Kim AMJ, Liu SSM, Yu J. Transdermal delivery of propranolol hydrochloride through chitosan nanoparticles dispersed in mucoadhesive gel. Carbohydr Polym. 2016;153:176–86. https://doi.org/10.1016/j.carbpol.2016.06.096.
91. Nawaz A, Wong TW. Microwave as skin permeation enhancer for transdermal drug delivery of chitosan-5-fluorouracil nanoparticles. Carbohydr Polym. 2017;157:906–19. https://doi.org/10.1016/j.carbpol.2016.09.080.
92. Ahmed TA, El-Say KM. Development of alginate-reinforced chitosan nanoparticles utilizing W/O nanoemulsification/internal crosslinking technique for transdermal delivery of rabeprazole. Life Sci. 2014;110(1):35–43. https://doi.org/10.1016/j.lfs.2014.06.019.
93. Vijayan V, Reddy KR, Sakthivel S, Swetha C. Optimization and charaterization of repaglinide biodegradable polymeric nanoparticle loaded transdermal patchs: in vitro and in vivo

studies. Colloids Surf B Biointerfaces. 2013;111:150–5. https://doi.org/10.1016/j.colsurfb.2013.05.020.
94. Aslam M, Aqil M, Ahad A, Najmi AK, Sultana Y, Ali A. Application of Box-Behnken design for preparation of glibenclamide loaded lipid based nanoparticles: optimization, in vitro skin permeation, drug release and in vivo pharmacokinetic study. J Mol Liq. 2016;219:897–908. https://doi.org/10.1016/j.molliq.2016.03.069.
95. Schneider M, Hirvonen J, Laaksonen T, Malinovskaja-Gomez K, Labouta HI. Transdermal iontophoresis of flufenamic acid loaded PLGA nanoparticles. Eur J Pharm Sci. 2016;89:154–62. https://doi.org/10.1016/j.ejps.2016.04.034.
96. Mennini N, Cirri M, Maestrelli F, Mura P. Comparison of liposomal and NLC (nanostructured lipid carrier) formulations for improving the transdermal delivery of oxaprozin: effect of cyclodextrin complexation. Int J Pharm. 2016;515(1–2):684–91. https://doi.org/10.1016/j.ijpharm.2016.11.013.
97. Santander-Ortega MJ, Stauner T, Loretz B, Ortega-Vinuesa JL, Bastos-González D, Wenz G, *et al*. Nanoparticles made from novel starch derivatives for transdermal drug delivery. J Control Release. 2010;141(1):85–92. https://doi.org/10.1016/j.jconrel.2009.08.012.
98. Joshi A, Kaur J, Kulkarni R, Chaudhari R. In-vitro and ex-vivo evaluation of raloxifene hydrochloride delivery using nano-transfersome based formulations. J Drug Deliv Sci Technol. 2018;45:151–8. https://doi.org/10.1016/j.jddst.2018.02.006.
99. Dutta K, Das B, Orasugh JT, Mondal D, Adhikari A, Rana D, *et al*. Bio-derived cellulose nanofibril reinforced poly(N-isopropylacrylamide)-g-guar gum nanocomposite: an avant-garde biomaterial as a transdermal membrane. Polymer. 2018;135:85–102. https://doi.org/10.1016/j.polymer.2017.12.015.
100. Fahmy UA, Aljaeid BM. Tadalafil transdermal delivery with alpha-lipoic acid self nanoemulsion for treatment of erectile dysfunction by diabetes mellitus. Int J Pharmacol. 2018;14(7):945–51. https://doi.org/10.3923/ijp.2018.945.951.
101. Zavgorodnya O, Penman AD, Bridges SL, Kharlampieva E, Carmona-Moran CA, Singh JA, *et al*. Development of gellan gum containing formulations for transdermal drug delivery: component evaluation and controlled drug release using temperature responsive nanogels. Int J Pharm. 2016;509(1–2):465–76. https://doi.org/10.1016/j.ijpharm.2016.05.062.
102. Saboktakin MR, Akhyari S, Nasirov FA. Synthesis and characterization of modified starch/polybutadiene as novel transdermal drug delivery system. Int J Biol Macromol. 2014;69:442–6. https://doi.org/10.1016/j.ijbiomac.2014.05.062.
103. Bose S, Du Y, Takhistov P, Michniak-Kohn B. Formulation optimization and topical delivery of quercetin from solid lipid based nanosystems. Int J Pharm. 2013;441(1–2):56–66. https://doi.org/10.1016/j.ijpharm.2012.12.013.
104. Tan JPK, Goh CH, Tam KC. Comparative drug release studies of two cationic drugs from pH-responsive nanogels. Eur J Pharm Sci. 2007;32(4–5):340–8. https://doi.org/10.1016/j.ejps.2007.08.010.
105. Mora L, Chumbimuni-Torres KY, Clawson C, Hernandez L, Zhang L, Wang J. Real-time electrochemical monitoring of drug release from therapeutic nanoparticles. J Control Release. 2009;140(1):69–73. https://doi.org/10.1016/j.jconrel.2009.08.002.
106. Wong TW, Nor KA. Physicochemical modulation of skin barrier by microwave for transdermal drug delivery. Pharm Res. 2013;30(1):90–103. https://doi.org/10.1007/s11095-012-0852-z.
107. Thermo Fisher Scientific USA. Slide-A-Lyzer™ MINI dialysis device, 10K MWCO, 2 mL https://www.thermofisher.com/order/catalog/product/88404. Accessed 20 Aug 2018.
108. Shahiwala A, Mehta T, Momin M. Parenteral drug delivery systems. In: Mishra A, Shahiwala A, editors. In-vitro and in-vivo tools in drug delivery research for optimum clinical outcomes. Florida: CRC; 2018.
109. Tan JPK, Tam KC. Application of drug selective electrode in the drug release study of pH-responsive microgels. J Control Release. 2007;118(1):87–94. https://doi.org/10.1016/j.jconrel.2006.11.017.
110. Rosenblatt KM, Douroumis D, Bunjes H. Drug release from differently structured monoolein/poloxamer nanodispersions studied with differential pulse polarography and ultrafiltration at low pressure. J Pharm Sci. 2007;96(6):1564–75. https://doi.org/10.1002/jps.20808.
111. Charalampopoulos N, Avgoustakis K, Kontoyannis CG. Differential pulse polarography: a suitable technique for monitoring drug release from polymeric nanoparticle dispersions. Anal Chim Acta. 2003;491(1):57–62. https://doi.org/10.1016/S0003-2670(03)00788-8.
112. Martin CA. Evaluating the utility of fiber optic analysis for dissolution testing of drug products. Dissolut Technol. 2003;10(4):37–9. https://doi.org/10.14227/DT100403P37.
113. Gray VA. Dissolution testing using fiber optics—a regulatory perspective. Dissolut Technol. 2003;10(4):33–6. https://doi.org/10.14227/DT100403P33.
114. Nir I, Lu X. In situ UV fiber optics for dissolution testing—what, why, and where we are after 30 years. Dissolution Technol. 2018;25(3):70–7. doi: https://doi.org/10.14227/DT250318P70
115. Guillot A, Limberge M, Krämer J, Lehr CM. In situ drug release monitoring with a fiber-optic system: overcoming matrix interferences using derivative spectrophotometry. Dissolut Technol. 2013;20(2):15–9. https://doi.org/10.14227/DT200213P15.
116. Uddin R, Saffoon N, Bishwajit S. Dissolution and dissolution apparatus: a review. Int J Curr Biomed Pharm Res. 2011;1(4):201–7. https://doi.org/10.1081/DDC-120021777.
117. Bijlani V, Yuonayel D, Katpally S, Chukwumezie BN, Adeyeye MC. Monitoring ibuprofen release from multiparticulates: in situ fiber-optic technique versus the HPLC method: a technical note. AAPS PharmSciTech. 2007;8(3):E9–12. https://doi.org/10.1208/pt0803052.
118. Voisine JM, Zolnik BS, Burgess DJ. In situ fiber optic method for long-term in vitro release testing of microspheres. Int J Pharm. 2008;356(1–2):206–11. https://doi.org/10.1016/J.IJPHARM.2008.01.017.
119. Liu L, Osei T, Hsu J, Greyling J. Evaluation of in-situ fiber optics dissolution method for compound A extended release tablets. Am Pharm Rev. 2011:1–9.
120. Romero EL, Morilla MJ. Ultradeformable phospholipid vesicles as a drug delivery system: a review. Res Rep Transderm Drug Deliv. 2015;4:55. https://doi.org/10.2147/rrtd.s50370.
121. Rizvi SAA, Saleh AM. Applications of nanoparticle systems in drug delivery technology. Saudi Pharm J. 2018;26(1):64–70. https://doi.org/10.1016/j.jsps.2017.10.012.
122. Jijie R, Barras A, Boukherroub R, Szunerits S. Nanomaterials for transdermal drug delivery: beyond the state of the art of liposomal structures. J Mater Chem B. 2017;5(44):8653–75. https://doi.org/10.1039/c7tb02529g.
123. Hoeller S, Sperger A, Valenta C. Lecithin based nanoemulsions: a comparative study of the influence of non-ionic surfactants and the cationic phytosphingosine on physicochemical behaviour and skin permeation. Int J Pharm. 2009;370(1–2):181–6. https://doi.org/10.1016/j.ijpharm.2008.11.014.
124. Klang V, Haberfeld S, Hartl A, Valenta C. Effect of γ-cyclodextrin on the in vitro skin permeation of a steroidal drug from nanoemulsions: impact of experimental setup. Int J Pharm. 2012;423(2):535–42. https://doi.org/10.1016/j.ijpharm.2011.11.037.
125. Raupach K, El-Hagin N, Valenta C, Klang V, Matsko N. Development of sucrose stearate-based nanoemulsions and optimisation through γ-cyclodextrin. Eur J Pharm Biopharm. 2011;79(1):58–67. https://doi.org/10.1016/j.ejpb.2011.01.010.
126. Biondi M, Cilurzo F, Campani V, De Rosa G, Mayol L, Pitaro M. Development of nanoemulsions for topical delivery of vitamin K1. Int J Pharm. 2016;511(1):170–7. https://doi.org/10.1016/j.ijpharm.2016.07.004.
127. Qi T, Qi-lu L, Guang-xi Z, Yan-wei X, Chen-yu G, Chun-fen Y, *et al*. Development of a quercetin-loaded nanostructured lipid carrier formulation for topical delivery. Int J Pharm. 2012;430(1–2):292–8. https://doi.org/10.1016/j.ijpharm.2012.03.042.
128. Zheng Y, Syed S, Hao C-S, Wang B-Z, Ouyang W-Q, Wei Y-P, *et al*. Effects of Carbopol® 934 proportion on nanoemulsion gel for topical and transdermal drug delivery: a skin permeation study. Int J Nanomedicine. 2016;11:5971–87. https://doi.org/10.2147/ijn.s119286.

129. Mazumder B, Ray S, Kaurav S, Ghosh S, Dasgupta S. In vitro & in vivo studies on lornoxicam loaded nanoemulsion gels for topical application. Curr Drug Deliv. 2014;11(1):132–8. https://doi.org/10.2174/15672018113106660063.
130. Kim BS, Won M, Lee KM, Kim CS. In vitro permeation studies of nanoemulsions containing ketoprofen as a model drug. Drug Deliv. 2008;15(7):465–9. https://doi.org/10.1080/10717540802328599.
131. Hussain Z, Katas H, Mohd Amin MCI, Kumolosasi E, Buang F, Sahudin S. Self-assembled polymeric nanoparticles for percutaneous co-delivery of hydrocortisone/hydroxytyrosol: an ex vivo and in vivo study using an NC/Nga mouse model. Int J Pharm. 2013;444(1–2):109–19. https://doi.org/10.1016/j.ijpharm.2013.01.024.
132. Akbari J, Saeedi M, Morteza-Semnani K, Rostamkalaei SS, Asadi M, Asare-Addo K, *et al*. The design of naproxen solid lipid nanoparticles to target skin layers. Colloids Surf B Biointerfaces. 2016;145:626–33. https://doi.org/10.1016/j.colsurfb.2016.05.064.
133. Abdel-Hafez SM, Hathout RM, Sammour OA. Tracking the transdermal penetration pathways of optimized curcumin-loaded chitosan nanoparticles via confocal laser scanning microscopy. Int J Biol Macromol. 2018;108:753–64. https://doi.org/10.1016/j.ijbiomac.2017.10.170.
134. Joshi SA, Jalalpure SS, Kempwade AA, Peram MR. Fabrication and in-vivo evaluation of lipid nanocarriers based transdermal patch of colchicine. J Drug Deliv Sci Technol. 2017;41:444–53. https://doi.org/10.1016/j.jddst.2017.08.013.
135. Anirudhan TS, Nair AS, Bino SJ. Nanoparticle assisted solvent selective transdermal combination therapy of curcumin and 5-flurouracil for efficient cancer treatment. Carbohydr Polym. 2017;173:131–42. https://doi.org/10.1016/j.carbpol.2017.05.045.
136. Ravikumar R, Ganesh M, Senthil V, Ramesh YV, Jakki SL, Choi EY. Tetrahydro curcumin loaded PCL-PEG electrospun transdermal nanofiber patch: preparation, characterization, and in vitro diffusion evaluations. J Drug Deliv Sci Technol. 2018;44:342–8. https://doi.org/10.1016/j.jddst.2018.01.016.
137. Ahmed TA, El-Say KM, Aljaeid BM, Fahmy UA, Abd-Allah FI. Transdermal glimepiride delivery system based on optimized ethosomal nano-vesicles: preparation, characterization, in vitro, ex vivo and clinical evaluation. Int J Pharm. 2016;500(1–2):245–54. https://doi.org/10.1016/j.ijpharm.2016.01.017.
138. Lin WJ, Duh YS. Nanostructured lipid carriers for transdermal delivery of acid labile lansoprazole. Eur J Pharm Biopharm. 2016;108:297–303. https://doi.org/10.1016/j.ejpb.2016.07.015.
139. Tsai MJ, Lu IJ, Fu YS, Fang YP, Huang YB, Wu PC. Nanocarriers enhance the transdermal bioavailability of resveratrol: in-vitro and in-vivo study. Colloids Surf B Biointerfaces. 2016;148:650–6. https://doi.org/10.1016/j.colsurfb.2016.09.045.
140. Aqil M, Moghaddam AA, Ahmad FJ, Ali A, Ahad A, Sultana Y. Ibuprofen loaded nano-ethanolic liposomes carbopol gel system: in vitro characterization and anti-inflammatory efficacy assessment in Wistar rats. J Polym Eng. 2017;38(3):291–8. https://doi.org/10.1515/polyeng-2016-0462.
141. Setya S, Razdan BK, Talegaonkar S, Tariq M, Madaan T. Appraisal of transdermal water-in-oil nanoemulgel of selegiline HCl for the effective management of Parkinson's disease: pharmacodynamic, pharmacokinetic, and biochemical investigations. AAPS PharmSciTech. 2018;19(2):573–89. https://doi.org/10.1208/s12249-017-0868-0.
142. Abdulbaqi IM, Darwis Y, Assi RA, Khan NAK. Transethosomal gels as carriers for the transdermal delivery of colchicine: statistical optimization, characterization, and ex vivo evaluation. Drug Des Devel Ther. 2018;12:795–813. https://doi.org/10.2147/DDDT.S158018.
143. Kaur A, Bhoop BS, Chhibber S, Sharma G, Gondil VS, Katare OP. Supramolecular nano-engineered lipidic carriers based on diflunisal-phospholipid complex for transdermal delivery: QbD based optimization, characterization and preclinical investigations for management of rheumatoid arthritis. Int J Pharm. 2017;533(1):206–24. https://doi.org/10.1016/j.ijpharm.2017.09.041.
144. Takeuchi I, Suzuki T, Makino K. Skin permeability and transdermal delivery route of 50-nm indomethacin-loaded PLGA nanoparticles. Colloids Surf B Biointerfaces. 2017;159:312–7. https://doi.org/10.1016/j.colsurfb.2017.08.003.
145. Qumbar M, Ameeduzzafar, Imam SS, Ali J, Ahmad J, Ali A. Formulation and optimization of lacidipine loaded niosomal gel for transdermal delivery: in-vitro characterization and in-vivo activity. Biomed Pharmacother. 2017;93:255–66. https://doi.org/10.1016/j.biopha.2017.06.043.
146. Sintov AC, Levy HV, Greenberg I. Continuous transdermal delivery of L-DOPA based on a self-assembling nanomicellar system. Pharm Res. 2017;34(7):1459–68. https://doi.org/10.1007/s11095-017-2162-y.
147. Arafa MG, Ayoub BM. DOE optimization of nano-based carrier of pregabalin as hydrogel: new therapeutic & chemometric approaches for controlled drug delivery systems. Sci Rep. 2017;7(1):41503. https://doi.org/10.1038/srep41503.
148. Xu H, Liu J, Yang X, Ni Q, Chen H, Hu W. Isotretinoin-loaded solid lipid nanoparticles with skin targeting for topical delivery. Int J Pharm. 2006;328(2):191–5. https://doi.org/10.1016/j.ijpharm.2006.08.007.
149. Trotta M, Peira E, Debernardi F, Gallarate M. Elastic liposomes for skin delivery of dipotassium glycyrrhizinate. Int J Pharm. 2002;241(2):319–27. https://doi.org/10.1016/S0378-5173(02)00266-1.
150. Alvarez-Román R, Naik A, Kalia YN, Guy RH, Fessi H. Enhancement of topical delivery from biodegradable nanoparticles. Pharm Res. 2004;21(10):1818–25. https://doi.org/10.1023/B:PHAM.0000045235.86197.ef.
151. Habib BA, Sayed S, Elsayed GM. Enhanced transdermal delivery of ondansetron using nanovesicular systems: fabrication, characterization, optimization and ex-vivo permeation study—Box-Cox transformation practical example. Eur J Pharm Sci. 2018;115:352–61. https://doi.org/10.1016/j.ejps.2018.01.044.
152. Pireddu R, Sinico C, Ennas G, Schlich M, Valenti D, Murgia S, *et al*. The effect of diethylene glycol monoethyl ether on skin penetration ability of diclofenac acid nanosuspensions. Colloids Surf B Biointerfaces. 2018;162:8–15. https://doi.org/10.1016/j.colsurfb.2017.11.012.
153. Ahad A, Al-Saleh AA, Al-Mohizea AM, Al-Jenoobi FI, Raish M, Yassin AEB, *et al*. Formulation and characterization of novel soft nanovesicles for enhanced transdermal delivery of eprosartan mesylate. Saudi Pharm J. 2017;25(7):1040–6. https://doi.org/10.1016/j.jsps.2017.01.006.
154. Alomrani AH, Badran MM. Flexosomes for transdermal delivery of meloxicam: characterization and antiinflammatory activity. Artif Cells Nanomed Biotechnol. 2017;45(2):305–12. https://doi.org/10.3109/21691401.2016.1147452.
155. Imam SS, Ahad A, Aqil M, Akhtar M, Sultana Y, Ali A. Formulation by design based risperidone nano soft lipid vesicle as a new strategy for enhanced transdermal drug delivery: in-vitro characterization, and in-vivo appraisal. Mater Sci Eng C. 2017;75:1198–205. https://doi.org/10.1016/j.msec.2017.02.149.
156. Butani D, Yewale C, Misra A. Topical amphotericin B solid lipid nanoparticles: design and development. Colloids Surf B Biointerfaces. 2016;139:17–24. https://doi.org/10.1016/j.colsurfb.2015.07.032.
157. Meng S, Zhang C, Shi W, Zhang X, Liu D, Wang P, *et al*. Preparation of osthole-loaded nano-vesicles for skin delivery: characterization, in vitro skin permeation and preliminary in vivo pharmacokinetic studies. Eur J Pharm Sci. 2016;92:49–54. https://doi.org/10.1016/j.ejps.2016.04.033.
158. Liu T, Niu X, Sun Q, Zhu Y, Wang XH, Wang L, *et al*. Evaluation of paeonol-loaded transethosomes as transdermal delivery carriers. Eur J Pharm Sci. 2017;99:240–5. https://doi.org/10.1016/j.ejps.2016.12.026.
159. Delgado-Charro MB, Guy RH. Effective use of transdermal drug delivery in children. Adv Drug Deliv Rev. 2014;73:63–82. https://doi.org/10.1016/j.addr.2013.11.014.
160. Michniak BB, Meidan V, Al-Khalili M, Wertz PW. Skin: physiology and penetration pathways. In: Meyer R, editor. Delivery system handbook for personal care and cosmetic products. Waltham: William Andrew-Elsevier; 2005. p. 77–100.

161. Cázares-Delgadillo J, Naik A, Kalia YN, Quintanar-Guerrero D, Ganem-Quintanar A. Skin permeation enhancement by sucrose esters: a pH-dependent phenomenon. Int J Pharm. 2005;297(1–2):204–12. https://doi.org/10.1016/j.ijpharm.2005.03.020.
162. Nair MK, Chetty DJ, Ho H, Chien YW. Biomembrane permeation of nicotine: mechanistic studies with porcine mucosae and skin. J Pharm Sci. 1997;86(2):257–62. https://doi.org/10.1021/js960095w.
163. Zorin S, Kuylenstierna F, Thulin H. In vitro test of nicotine's permeability through human skin. Risk evaluation and safety aspects. Ann Occup Hyg. 1999;43(6):405–13. https://doi.org/10.1016/S0003-4878(99)00030-7.
164. Heard CM, Johnson S, Moss G, Thomas CP. In vitro transdermal delivery of caffeine, theobromine, theophylline and catechin from extract of guarana, *Paullinia cupana*. Int J Pharm. 2006;317(1):26–31. https://doi.org/10.1016/j.ijpharm.2006.02.042.
165. Chen L, Han L, Lian G. Recent advances in predicting skin permeability of hydrophilic solutes. Adv Drug Deliv Rev. 2013;65(2):295–305. https://doi.org/10.1016/j.addr.2012.05.001.
166. Lehman PA, Raney SG, Franz TJ. Percutaneous absorption in man: in vitro-in vivo correlation. Skin Pharmacol Physiol. 2011;24(4):224–30. https://doi.org/10.1159/000324884.
167. Williams AC, Barry BW. Penetration enhancers. Adv Drug Deliv Rev. 2012;64(SUPPL):128–37. https://doi.org/10.1016/j.addr.2012.09.032.
168. Azarmi S, Roa W, Löbenberg R. Current perspectives in dissolution testing of conventional and novel dosage forms. Int J Pharm. 2007;328(1 SPEC. ISS):12–21. https://doi.org/10.1016/j.ijpharm.2006.10.001.
169. Gillet A, Evrard B, Piel G. Liposomes and parameters affecting their skin penetration behaviour. J Drug Deliv Sci Technol. 2011;21(1):35–42. https://doi.org/10.1016/S1773-2247(11)50004-8.
170. Organisation for Economic Co-operation and Development (OECD). Joint meeting of the chemicals committee and the working party on chemicals, pesticides and biotechnology guidance notes on dermal absorption series on testing and assessment no. 156. ENV/JM/MONO(2011)36. 2011. https://www.oecd.org/chemicalsafety/testing/48532204.pdf. Accessed 10 Nov 2018.
171. Sartorelli P, Andersen HR, Angerer J, Corish J, Drexler H, Göen T, *et al*. Percutaneous penetration studies for risk assessment. Environ Toxicol Pharmacol. 2000;8(2):133–52. https://doi.org/10.1016/S1382-6689(00)00035-1.
172. Bronaugh R. Methods for in vitro percutaneous absorption. In: Zhai H, Maibach H, editors. Dermatotoxicology. New York: CRC; 2004. p. 520–6.
173. Roussel L, Abdayem R, Gilbert E, Pirot F, Haftek M. Influence of excipients on two elements of the stratum corneum barrier: intercellular lipids and epidermal tight junctions. In: Percutaneous penetration enhancers chemical methods in penetration enhancement: drug manipulation strategies and vehicle effects. Berlin: Springer; 2015. p. 69–92. https://doi.org/10.1007/978-3-662-45013-0_7.
174. Duan J, Seo P, Shah H, Suarez-Sharp S, Li M. Regulatory experience with in vivo in vitro correlations (IVIVC) in new drug applications. AAPS J. 2016;18(6):1379–90. https://doi.org/10.1208/s12248-016-9966-2.
175. Park K. Translation from mouse to human: time to think in new boxes. J Control Release. 2014;189:187. https://doi.org/10.1016/j.jconrel.2014.07.046.
176. Cardot JM, Beyssac E, Alric M. In vitro–in vivo correlation: importance of dissolution in IVIVC. Dissolut Technol. 2007;14(1):15–9. https://doi.org/10.14227/DT140107P15.
177. Sakore S, Chakraborty B. In vitro-in vivo correlation (IVIVC): a strategic tool in drug development. J Bioequiv Availab. 2011;8(4). https://doi.org/10.4172/jbb.S3-001.
178. Kumar R, Nagarwal RC, Dhanawat M, Pandit JK. In-vitro and in-vivo study of indomethacin loaded gelatin nanoparticles. J Biomed Nanotechnol. 2011;7(3):325–33. https://doi.org/10.1166/jbn.2011.1290.
179. Cao X, Deng WW, Fu M, Wang L, Tong SS, Wei YW, *et al*. In vitro release and in vitro-in vivo correlation for silybin meglumine incorporated into hollow-type mesoporous silica nanoparticles. Int J Nanomedicine. 2012;7:753–62. https://doi.org/10.2147/IJN.S28348.
180. Tiwari R, Pathak K. Nanostructured lipid carrier versus solid lipid nanoparticles of simvastatin: comparative analysis of characteristics, pharmacokinetics and tissue uptake. Int J Pharm. 2011;415(1–2):232–43. https://doi.org/10.1016/j.ijpharm.2011.05.044.
181. Huang Q, Li XM, Wei P, Wang Y, Chen B, Chen W, *et al*. Study on the release of fenofibrate nanosuspension in vitro and its correlation with in situ intestinal and in vivo absorption kinetics in rats. Drug Dev Ind Pharm. 2014;40(7):972–9. https://doi.org/10.3109/03639045.2013.794828.
182. Pavurala N, Khan MA, Krishnaiah YSR, Yang Y, Manda P. Development and validation of in vitro–in vivo correlation (IVIVC) for estradiol transdermal drug delivery systems. J Control Release. 2015;210:58–66. https://doi.org/10.1016/j.jconrel.2015.05.263.
183. Tirumalasetty PP, Mutalik S, Pillai R, Kondamudi PK, Malayandi R. Lidocaine transdermal patch: pharmacokinetic modeling and in vitro-in vivo correlation (IVIVC). AAPS PharmSciTech. 2016;17(3):588–96. https://doi.org/10.1208/s12249-015-0390-1.
184. Yan K, Yan T, Guo H, Li J, Wei L. Evaluation of transdermal permeability of pentoxifylline gel: in vitro skin permeation and in vivo microdialysis using Wistar rats. Drug Discov Ther. 2007;1(1):78–83.
185. Shen J, Burgess DJ. In vitro-in vivo correlation for complex non-oral drug products: where do we stand? J Control Release. 2015;219:644–51. https://doi.org/10.1016/j.jconrel.2015.09.052.